USGS
science for a changing world

Gallium

Chapter H of

Critical Mineral Resources of the United States—Economic and Environmental Geology and Prospects for Future Supply

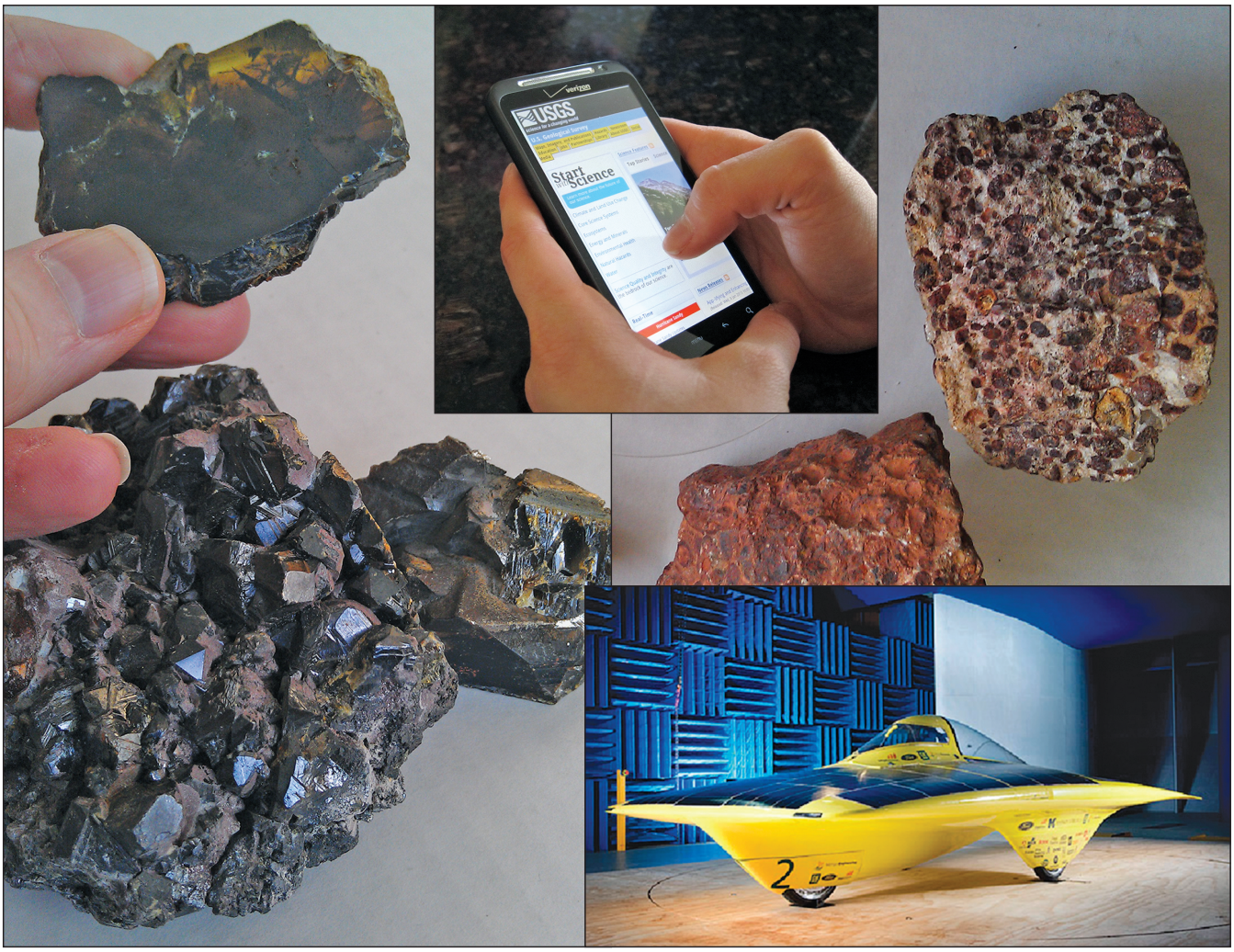

Professional Paper 1802–H

U.S. Department of the Interior
U.S. Geological Survey

Periodic Table of Elements

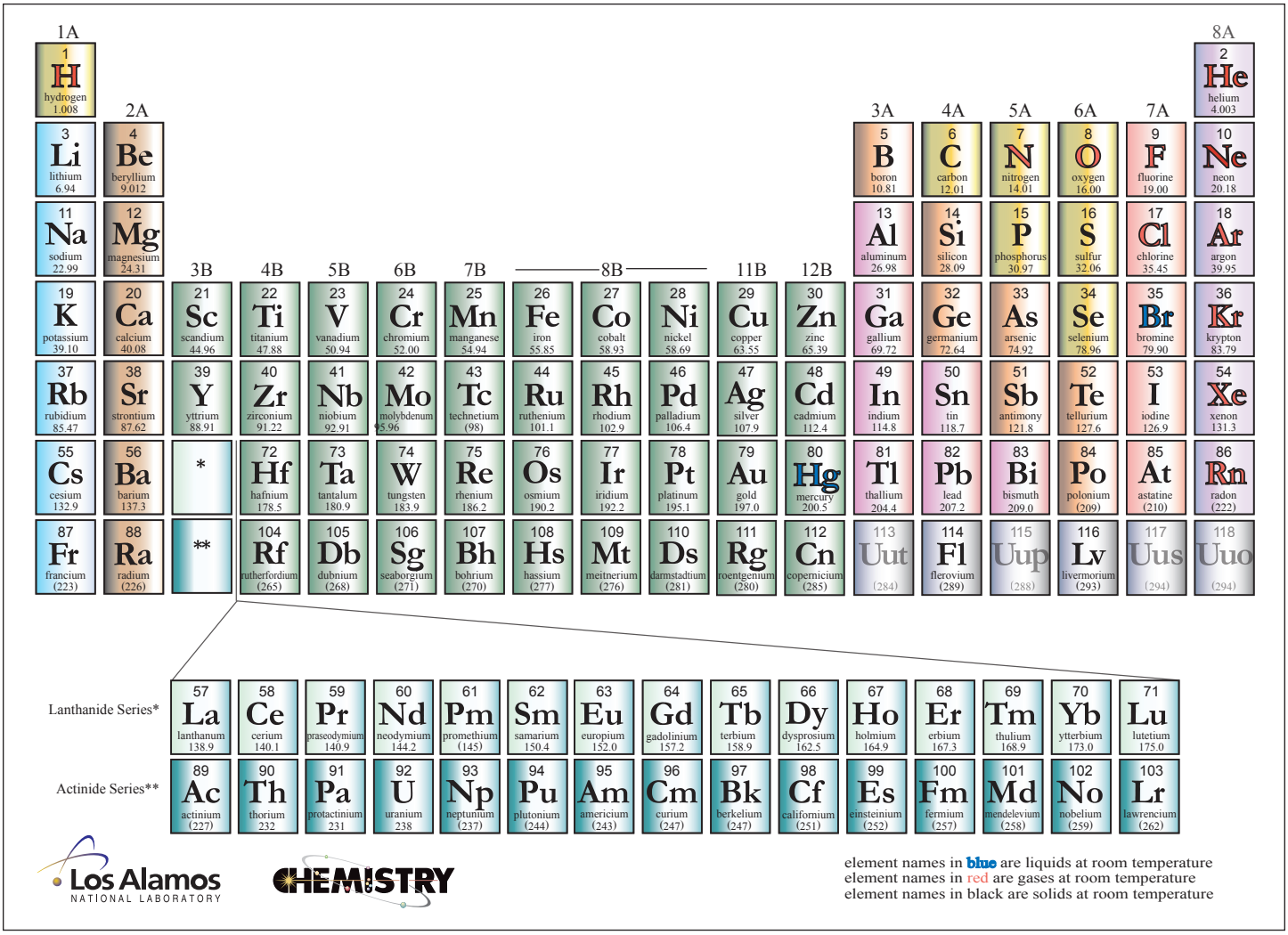

Modified from Los Alamos National Laboratory Chemistry Division; available at http://periodic.lanl.gov/images/periodictable.pdf.

Cover. Photographs showing samples of bauxite ore and sphalerite ore, which are the primary mineralogical sources of gallium. Gallium is used in a variety of products from smartphones to experimental cars, also shown. Photograph of experimental car courtesy of the University of Michigan; used with permission.

Gallium

By Nora K. Foley, Brian W. Jaskula, Bryn E. Kimball, and Ruth F. Schulte

Chapter H of

Critical Mineral Resources of the United States—Economic and Environmental Geology and Prospects for Future Supply

Edited by Klaus J. Schulz, John H. DeYoung, Jr., Robert R. Seal II, and Dwight C. Bradley

Professional Paper 1802–H

U.S. Department of the Interior
U.S. Geological Survey

U.S. Department of the Interior
RYAN K. ZINKE, Secretary

U.S. Geological Survey
William H. Werkheiser, Acting Director

U.S. Geological Survey, Reston, Virginia: 2017

Suggested citation:
Foley, N.K., Jaskula, B.W., Kimball, B.E., and Schulte, R.F., 2017, Gallium, chap. H *of* Schulz, K.J., DeYoung, J.H., Jr., Seal, R.R., II, and Bradley, D.C., eds., Critical mineral resources of the United States—Economic and environmental geology and prospects for future supply: U.S. Geological Survey Professional Paper 1802, p. H1–H35, https://doi.org/10.3133/pp1802H.

ISSN 2330-7102 (online)

Contents

Figures

Tables

Conversion Factors

International System of Units to Inch/Pound

Multiply	By	To obtain
	Length	
angstrom (Å) (0.1 nanometer)	0.003937	microinch
angstrom (Å) (0.1 nanometer)	0.000003937	mil
micrometer (µm) [or micron]	0.03937	mil
millimeter (mm)	0.03937	inch (in.)
centimeter (cm)	0.3937	inch (in.)
meter (m)	3.281	foot (ft)
meter (m)	1.094	yard (yd)
kilometer (km)	0.6214	mile (mi)
	Area	
hectare (ha)	2.471	acre
square kilometer (km^2)	247.1	acre
square meter (m^2)	10.76	square foot (ft^2)
square centimeter (cm^2)	0.1550	square inch (ft^2)
square kilometer (km^2)	0.3861	square mile (mi^2)
	Volume	
milliliter (mL)	0.03381	ounce, fluid (fl. oz)
liter (L)	33.81402	ounce, fluid (fl. oz)
liter (L)	1.057	quart (qt)
liter (L)	0.2642	gallon (gal)
cubic meter (m^3)	264.2	gallon (gal)
cubic centimeter (cm^3)	0.06102	cubic inch (in^3)
cubic meter (m^3)	1.308	cubic yard (yd^3)
cubic kilometer (km^3)	0.2399	cubic mile (mi^3)
	Mass	
microgram (µg)	0.00000003527	ounce, avoirdupois (oz)
milligram (mg)	0.00003527	ounce, avoirdupois (oz)
gram (g)	0.03527	ounce, avoirdupois (oz)
gram (g)	0.03215075	ounce, troy
kilogram (kg)	32.15075	ounce, troy
kilogram (kg)	2.205	pound avoirdupois (lb)
ton, metric (t)	1.102	ton, short [2,000 lb]
ton, metric (t)	0.9842	ton, long [2,240 lb]
	Deposit grade	
gram per metric ton (g/t)	0.0291667	ounce per short ton (2,000 lb) (oz/T)
	Pressure	
megapascal (MPa)	10	bar
gigapascal (GPa)	10,000	bar
	Density	
gram per cubic centimeter (g/cm^3)	62.4220	pound per cubic foot (lb/ft^3)
milligram per cubic meter (mg/m^3)	0.00000006243	pound per cubic foot (lb/ft^3)
	Energy	
joule (J)	0.0000002	kilowatthour (kWh)
joule (J)	6.241×10^{18}	electronvolt (eV)
joule (J)	0.2388	calorie (cal)
kilojoule (kJ)	0.0002388	kilocalorie (kcal)

International System of Units to Inch/Pound—Continued

Multiply	By	To obtain
	Radioactivity	
becquerel (Bq)	0.00002703	microcurie (μCi)
kilobecquerel (kBq)	0.02703	microcurie (μCi)
	Electrical resistivity	
ohm meter (Ω-m)	39.37	ohm inch (Ω-in.)
ohm-centimeter (Ω-cm)	0.3937	ohm inch (Ω-in.)
	Thermal conductivity	
watt per centimeter per degree Celsius (watt/cm °C)	693.1798	International British thermal unit inch per hour per square foot per degree Fahrenheit (Btu in/h ft^2 °F)
watt per meter kelvin (W/m-K)	6.9318	International British thermal unit inch per hour per square foot per degree Fahrenheit (Btu in/h ft^2 °F)

Inch/Pound to International System of Units

	Length	
mil	25.4	micrometer (μm) [or micron]
inch (in.)	2.54	centimeter (cm)
inch (in.)	25.4	millimeter (mm)
foot (ft)	0.3048	meter (m)
mile (mi)	1.609	kilometer (km)
	Volume	
ounce, fluid (fl. oz)	29.57	milliliter (mL)
ounce, fluid (fl. oz)	0.02957	liter (L)
	Mass	
ounce, avoirdupois (oz)	28,350,000	microgram
ounce, avoirdupois (oz)	28,350	milligram
ounce, avoirdupois (oz)	28.35	gram (g)
ounce, troy	31.10 348	gram (g)
ounce, troy	0.03110348	kilogram (kg)
pound, avoirdupois (lb)	0.4536	kilogram (kg)
ton, short (2,000 lb)	0.9072	ton, metric (t)
ton, long (2,240 lb)	1.016	ton, metric (t)
	Deposit grade	
ounce per short ton (2,000 lb) (oz/T)	34.285714	gram per metric ton (g/t)
	Energy	
kilowatthour (kWh)	3,600,000	joule (J)
electronvolt (eV)	1.602×10^{-19}	joule (J)
	Radioactivity	
microcurie (μCi)	37,000	becquerel (Bq)
microcurie (μCi)	37	kilobecquerel (kBq)

Temperature in degrees Celsius (°C) may be converted to degrees Fahrenheit (°F) as follows:

$$°F = (1.8 \times °C) + 32$$

Temperature in degrees Celsius (°C) may be converted to kelvin (K) as follows:

$$K = °C + 273.15$$

Temperature in degrees Fahrenheit (°F) may be converted to degrees Celsius (°C) as follows:

$$°C = (°F - 32) / 1.8$$

Datum

Unless otherwise stated, vertical and horizontal coordinate information is referenced to the World Geodetic System of 1984 (WGS 84). Altitude, as used in this report, refers to distance above the vertical datum.

Supplemental Information

Specific conductance is given in microsiemens per centimeter at 25 degrees Celsius (µS/cm at 25 °C).

Concentrations of chemical constituents in soils and (or) sediment are given in milligrams per kilogram (mg/kg), parts per million (ppm), or parts per billion (ppb).

Concentrations of chemical constituents in water are given in milligrams per liter (mg/L), micrograms per liter (µg/L), nanogams per liter (ng/L), nanomoles per kilogram (nmol/kg), parts per million (ppm), parts per billion (ppb), or parts per trillion (ppt).

Concentrations of suspended particulates in water are given in micrograms per gram (µg/g), milligrams per kilogram (mg/kg), or femtograms per gram (fg/g).

Concentrations of chemicals in air are given in units of the mass of the chemical (milligrams, micrograms, nanograms, or picograms) per volume of air (cubic meter).

Activities for radioactive constituents in air are given in microcuries per milliliter (µCi/mL).

Deposit grades are commonly given in percent, grams per metric ton (g/t)—which is equivalent to parts per million (ppm)—or troy ounces per short ton (oz/T).

Geologic ages are expressed in mega-annum (Ma, million years before present, or 10^6 years ago) or giga-annum (Ga, billion years before present, or 10^9 years ago).

For ranges of years, "to" and (or) the en dash ("–") mean "up to and including."

Concentration unit	Equals
milligram per kilogram (mg/kg)	part per million
microgram per gram (µg/g)	part per million
microgram per kilogram (µg/kg)	part per billion (10^9)

Equivalencies

part per million (ppm): 1 ppm = 1,000 ppb = 1,000,000 ppt = 0.0001 percent
part per billion (ppb): 0.001 ppm = 1 ppb = 1,000 ppt = 0.0000001 percent
part per trillion (ppt): 0.000001 ppm = 0.001 ppb = 1 ppt = 0.0000000001 percent

Metric system prefixes

tera- (T-)	10^{12}	1 trillion
giga- (G-)	10^9	1 billion
mega- (M-)	10^6	1 million
kilo- (k-)	10^3	1 thousand
hecto- (h-)	10^2	1 hundred
deka- (da-)	10	1 ten
deci- (d-)	10^{-1}	1 tenth
centi- (c-)	10^{-2}	1 hundredth
milli- (m-)	10^{-3}	1 thousandth
micro- (µ-)	10^{-6}	1 millionth
nano- (n-)	10^{-9}	1 billionth
pico- (p-)	10^{-12}	1 trillionth
femto- (f-)	10^{-15}	1 quadrillionth
atto- (a-)	10^{-18}	1 quintillionth

Abbreviations and Symbols

°C	degree Celsius
µg/L	microgram per liter
µg Al/L	microgram of aluminum per liter
µg Mn/m^3	microgram of manganese per cubic meter
µg Mn/L	microgram of manganese per liter
Å	angstrom
AMD	acid mine drainage
ATSDR	Agency for Toxic Substances and Disease Registry
CIGS	copper-indium-gallium-(di)selenide
g CO_2-equiv/kWh	gram of CO_2 equivalent per kilowatthour
LC_{50}	lethal concentration 50 (concentration that kills 50 percent of test population within a given timeframe)
LED	light-emitting diode
Ma	mega-annum
mg Al/kg	milligram of aluminum per kilogram
mg/kg	milligram per kilogram
mg/L	milligram per liter
mm	millimeter
ng/m^3	nanogram per cubic meter
OSHA	Occupational Safety and Health Administration
ppm	part per million
RF	radio-frequency
SAF	submerged-arc furnace
USGS	U.S. Geological Survey

Gallium

By Nora K. Foley, Brian W. Jaskula, Bryn E. Kimball, and Ruth F. Schulte

Abstract

Gallium is a soft, silvery metallic element with an atomic number of 31 and the chemical symbol Ga. Gallium is used in a wide variety of products that have microelectronic components containing either gallium arsenide (GaAs) or gallium nitride (GaN). GaAs is able to change electricity directly into laser light and is used in the manufacture of optoelectronic devices (laser diodes, light-emitting diodes [LEDs], photo detectors, and solar cells), which are important for aerospace and telecommunications applications and industrial and medical equipment. GaAs is also used in the production of highly specialized integrated circuits, semiconductors, and transistors; these are necessary for defense applications and high-performance computers. For example, cell phones with advanced personal computer-like functionality (smartphones) use GaAs-rich semiconductor components. GaN is used principally in the manufacture of LEDs and laser diodes, power electronics, and radio-frequency electronics. Because GaN power transistors operate at higher voltages and with a higher power density than GaAs devices, the uses for advanced GaN-based products are expected to increase in the future. Gallium technologies also have large power-handling capabilities and are used for cable television transmission, commercial wireless infrastructure, power electronics, and satellites. Gallium is also used for such familiar applications as screen backlighting for computer notebooks, flat-screen televisions, and desktop computer monitors.

Gallium is dispersed in small amounts in many minerals and rocks where it substitutes for elements of similar size and charge, such as aluminum and zinc. For example, gallium is found in small amounts (about 50 parts per million) in such aluminum-bearing minerals as diaspore-boehmite and gibbsite, which form bauxite deposits, and in the zinc-sulfide mineral sphalerite, which is found in many mineral deposits. At the present time, gallium metal is derived mainly as a byproduct of the processing of bauxite ore for aluminum; lesser amounts of gallium metal are produced from the processing of sphalerite ore from three types of deposits (sediment-hosted, Mississippi Valley-type, and volcanogenic massive sulfide) for zinc. The United States is expected to meet its current and expected future needs for gallium through imports of primary, recycled, and refined gallium, as well as through domestic production of recycled and refined gallium. The U.S. Geological Survey estimates that world resources of gallium in bauxite exceed 1 billion kilograms, and a considerable quantity of gallium could be present in world zinc reserves.

Introduction

The existence of gallium was first predicted in 1871 by Dmitri Mendeleev, a Russian chemist who published the first periodic table of elements (Mendeleev, 1871). Mendeleev noted a gap in his table and named the missing element "eka-aluminum" because he determined that its location was one place away from aluminum in the table (fig. H1). Mendeleev thought that the missing element (gallium) would be

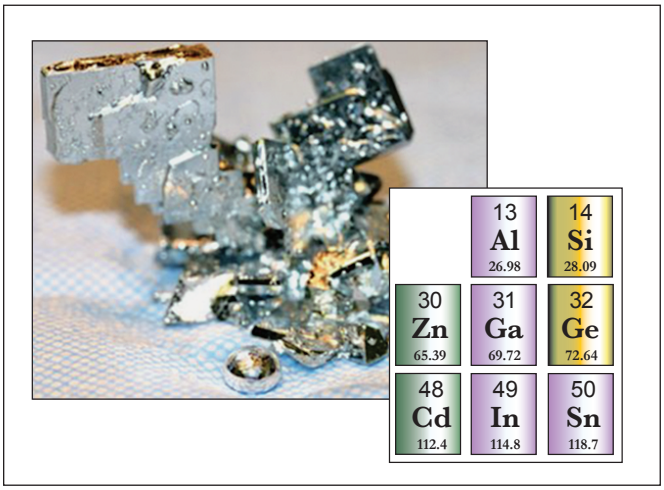

Figure H1. Photograph of gallium metal with an inset showing its position on the periodic table of elements. The gallium crystals shown in the photograph grew in a tank of liquid gallium. The drop in the foreground fell off the crystal as the liquid slowly cooled below a temperature of about 30 degrees Celsius. Photograph courtesy of Afshin Yaghmaei, Simulated Planetary Interiors Lab, Department of Earth and Space Sciences, University of California, Los Angeles.

very much like aluminum in its chemical properties, and he was right. The French chemist Paul-Emile Lecoq de Boisbaudran discovered gallium in sphalerite in 1875 using spectroscopy. Lecoq de Boisbaudran isolated gallium metal by electrolysis of gallium hydroxide in a potassium hydroxide solution. He named the element "gallia" after the Latin name for his native land of France (*Gallia*, or Gaul).

Solid gallium has a low melting temperature (about 29 degrees Celsius [°C]) and an unusually high boiling point (about 2,204 °C) (table H1), so that gallium is a liquid across a wider range of temperatures than any other element. Because of these properties, the earliest uses of gallium were in high-temperature thermometry and in metal alloys that melt easily. The development of gallium arsenide as a direct band-gap semiconductor in the 1960s led to what are now some of the most well-known uses of gallium—in feature-rich, application-intensive, third- and fourth-generation smartphones and in data-centric networks.

Strategic and Critical Resource Issues

Gallium first became recognized as a strategic and critical metal during World War II because it was a necessary component of a stable gallium-plutonium alloy that was developed as part of the Manhattan Project and used to make a reliable atomic bomb. Gallium is currently important for U.S. manufacturing because of its expanding uses for novel thin-film photovoltaics, especially those of the copper-indium-gallium-(di)selenide (CIGS) semiconductor type, and it is particularly important for clean energy technologies. Gallium is currently produced as a byproduct of the mining of other mineral commodities—mainly zinc, copper, and aluminum—and the mining technologies used are optimized for the extraction of those primary mineral commodities. The small market for gallium as a specialty metal creates little incentive for refiners of zinc, copper, and aluminum ores to invest in improvements to increase byproduct recovery of gallium. Because of the likelihood of rapid growth in the areas of photovoltaics and clean energy technologies, a potential exists for bottlenecks in the gallium supply pipeline. Production of gallium is limited by market factors that influence the production of the principal mineral commodity, whether it is zinc or aluminum.

Uses and Applications

A wide variety of products have microelectronic components that contain either gallium arsenide (GaAs) or gallium nitride (GaN). GaAs is able to change electricity directly into laser light and is used in the manufacture of optoelectronic devices (laser diodes, light-emitting diodes [LEDs], photo detectors, and solar cells), which are important for aerospace and telecommunications applications and industrial and medical equipment. GaAs is also used in the production of highly specialized integrated circuits, semiconductors, and transistors; these are necessary for defense applications and high-performance computers. For example, smartphones (cell phones with advanced computer-like functionality) use GaAs-rich semiconductor components (fig. H2*A*). GaN is employed principally in the manufacture of LEDs and laser diodes, power electronics, and radio-frequency (RF) electronics. Because GaN power transistors operate at higher voltages and with a higher power density than GaAs devices, the applications for advanced GaN-based products are expected to increase in the future. The CIGS direct band-gap semiconductor was developed to make lightweight, flexible, and durable thin-film photovoltaics that have a high absorption coefficient; these attributes have potential applications in the manufacture of efficient solar cells (fig. H2*B*). Because of its high boiling temperature, gallium is used to make thermometers designed to measure very high temperatures, and because of its silvery color and ability to form metal alloys, gallium is used to make brilliant mirrors. The fundamental properties of thermal convection in liquid gallium metal are employed to study aspects of planetary and astrophysical magnetohydrodynamics.

Gallium can be replaced by other materials in some applications, but for others, it has no effective substitutes. Liquid crystals made from organic compounds are used in visual displays as substitutes for LEDs. Researchers also are working to develop organic-based LEDs that may compete with GaAs in the future. Indium phosphide components can be substituted for GaAs-based infrared laser diodes in some specific-wavelength applications, and helium-neon lasers can be used in place of GaAs lasers in visible laser diode applications. Silicon is the principal competitor with GaAs in solar-cell applications. GaAs-based integrated circuits are used in many defense-related applications because of their unique properties, and there are no effective substitutes for GaAs in these applications. GaAs in heterojunction bipolar transistors is being substituted by silicon-germanium in some applications.

In 2012, imports of gallium and GaAs wafers, which were valued at about $32 million, continued to satisfy almost all U.S. demand for gallium. GaAs and GaN electronic components represented about 99 percent of domestic gallium consumption (fig. H3). About 70 percent of the gallium was used in integrated circuits (both analog and digital), including those in defense applications, high-performance computers, and telecommunications. Optoelectronic devices for use in aerospace and telecommunications applications, consumer goods, industrial equipment, medical equipment, and so forth, as well as a small amount for research and development, represented the remaining 30 percent of gallium consumption.

Gallium prices decreased throughout 2012 when significant increases in gallium production from 2007 to 2012 (fig. H4) exceeded the declining demand from LED producers. Gallium production capacity in China

expanded tremendously from 2008 to 2012 on the expectation of a strong LED-based backlighting market, which failed to materialize. In January 2012, the price for low-grade gallium metal (with a purity of 99.099 percent compared with a purity of 99.99999 for the higher grade) averaged $580 per kilogram. By July, the average price for low-grade gallium metal had decreased to $320 per kilogram, and by early October, to $280 per kilogram.

Markets continued to expand for GaAs- and GaN-based products in 2012. GaAs demand mainly results from cell phones and other high-speed wireless applications. In 2012, GaAs demand increased owing to the rapid increase in the use of feature-rich, application-intensive, third- and fourth-generation smartphones, which contain up to 10 times the amount of GaAs compared with standard cellular handsets. Smartphones accounted for 37 percent of all handsets sold in 2012. Owing to the increased amounts of GaAs in smartphones and the increased use of GaAs-based LEDs in general lighting and automotive applications, the value of sales in the GaAs market is forecast to reach $650 million by 2017 at an annual growth rate of nearly 11 percent (Jaskula, 2013b).

Owing to the large power-handling capabilities, high-switching frequencies, and higher voltage capabilities of GaN technology, GaN-based products, which historically have been used in defense and military applications, have begun to gain acceptance in the cable television transmission, commercial wireless infrastructure, power electronics, and satellite markets. The value of sales for the GaN power device market was expected to reach $178 million by 2015 at an annual growth rate of nearly 29 percent (Jaskula, 2013b).

In 2012, the worldwide LED market, which was a significant driver for GaN-based technologies, increased by only 1.5 percent in revenues from that of 2011 owing to slower-than-expected growth in the LED backlighting market and to lower LED prices, as production was outpacing demand. Although televisions were increasingly being built with LED backlighting in 2012, improvements in technology required up to 50 percent fewer LEDs. LED-backlit televisions accounted for 63 percent of the television market in 2012 and were forecast to account for 93 percent of market sales in 2013. By 2014, the strongest market segments for sales of LEDs were expected to be in general lighting, followed by signs and automotive applications.

Sustained high prices for energy continued to spark interest in solar energy in 2012. Sales of CIGS semiconductors for use in the production of high-efficiency solar cells was slower than expected, however, owing to a complicated manufacturing process that has impeded commercial mass production of CIGS panels. Decreased prices of silicon-based solar cells also affected demand for the more expensive CIGS technology. These two factors resulted in a large oversupply of CIGS modules that caused prices to decrease by 20 percent in 2011 and to remain low throughout 2012. In an effort to keep CIGS technology viable and competitive, CIGS manufacturers began in 2011 to trim production costs, improve module conversion efficiencies, and increase the use of CIGS-based photovoltaics in commercial rooftops.

The following sections of this chapter provide an overview of the principal types and global distribution of domestic and global resources of gallium (fig. H4). This information updates the report by Weeks (1973).

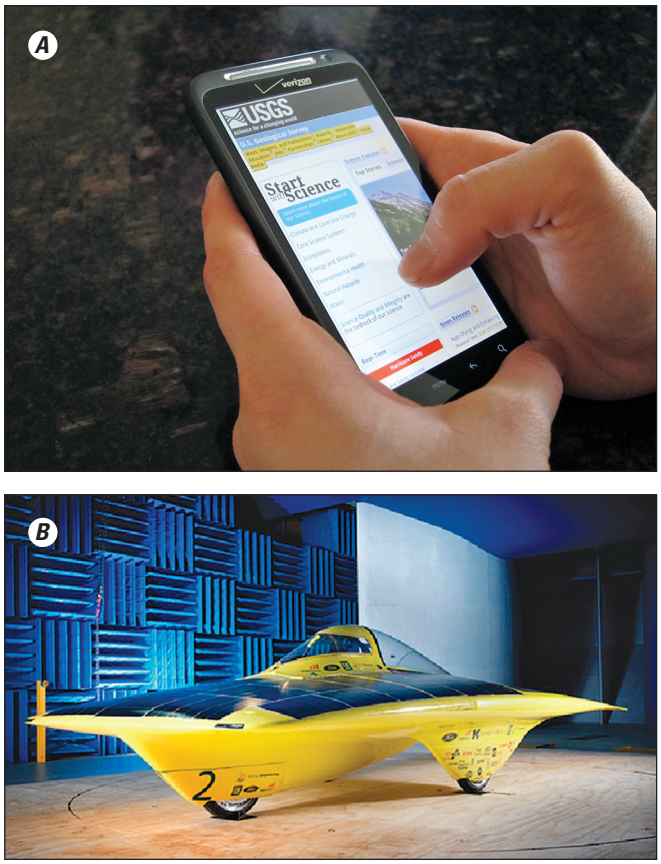

Figure H2. Photographs showing examples of some current uses for gallium. *A*, Cell phone that has advanced computer-like functionality (that is, a smartphone), which contains gallium-based semiconductor components and, consequently, up to 10 times the amount of gallium arsenide (GaAs) than is used in standard cell phones. *B*, Experimental three-wheel car displaying high-efficiency, triple-junction GaAs solar cells. Such solar cells have many experimental applications; this three-wheel car, the Continuum, which was built at the University of Michigan, weighs 220 kilograms and is covered with about 2,500 aerospace-grade GaAs-type solar cells. Photograph of experimental car courtesy of the University of Michigan.

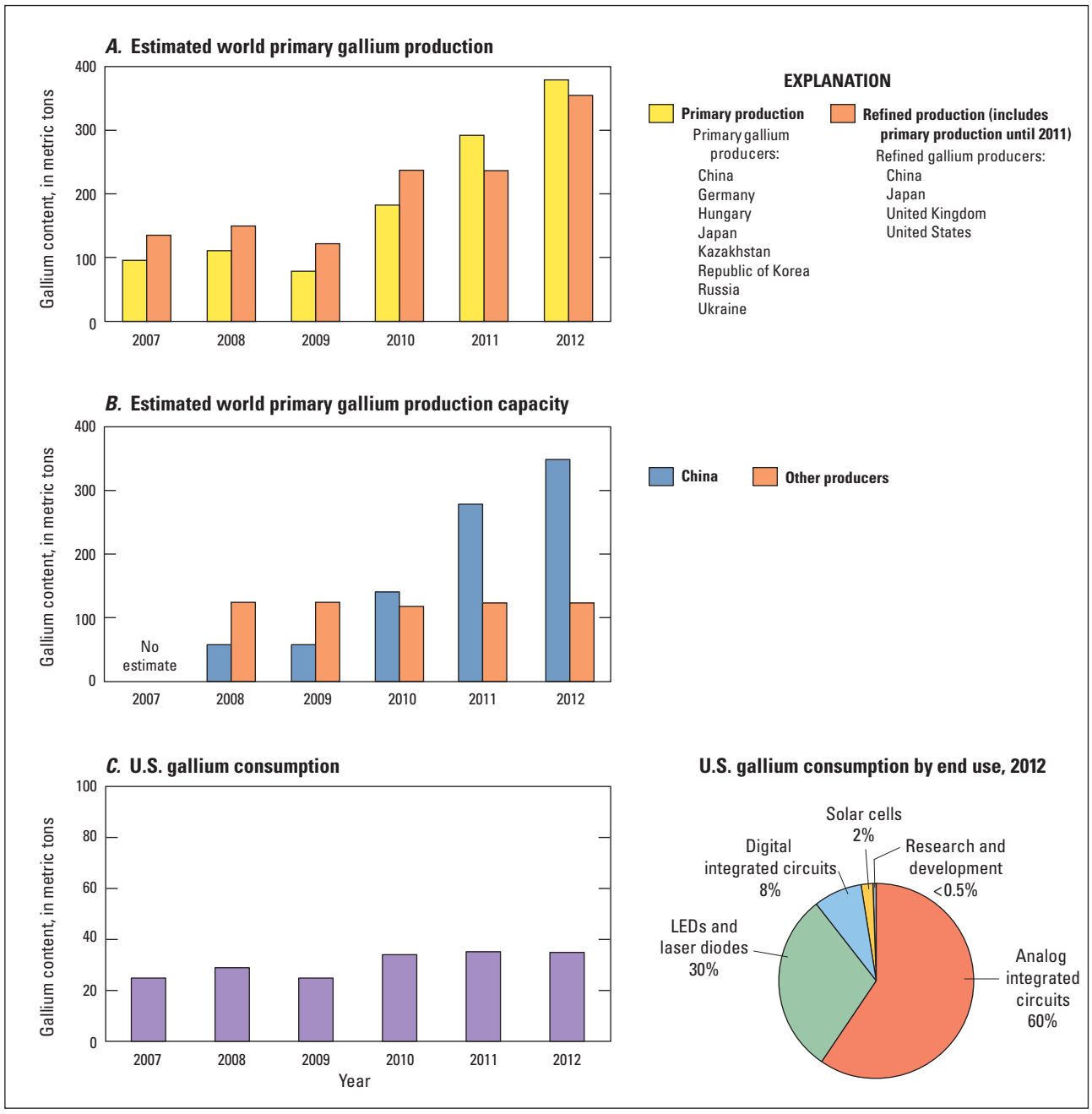

Figure H3. Charts showing U.S. and world gallium production and consumption from 2007 to 2012. *A*, Estimated world primary gallium production and refined gallium production from 2007 to 2012. *B*, Estimated world primary gallium production capacity for China and the rest of the world from 2008 to 2012. *C*, Gallium consumption in the United States from 2007 to 2012, and major end uses of gallium as a percentage of U.S. consumption in 2012. Percentages in the pie chart have been rounded and consequently do not add to 100. LEDs, light-emitting diodes

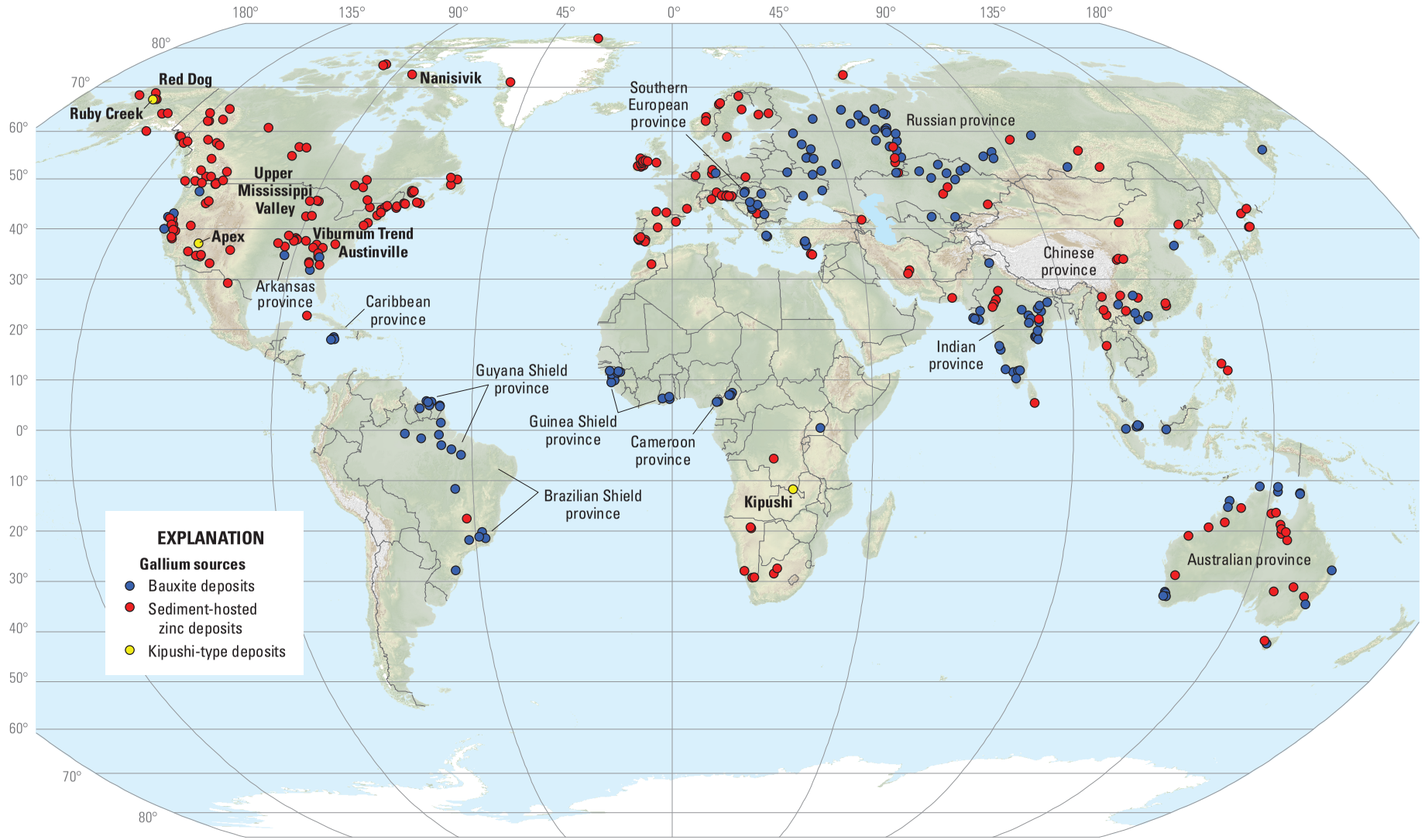

Base from U.S. Geological Survey Global 30 arc-second elevation data (1996) and from Natural Earth (2014); Robinson projection; World Geodetic System 1984 datum

Figure H4. World map showing locations of selected mineral deposits, by type; gallium has been produced from these types of deposits. The selected bauxite deposits are located within the world's major bauxite provinces and include both karst and lateritic types. The sediment-hosted zinc deposits and districts named in the text (Austinville, Nanisivik, Red Dog, Ruby Creek, and Viburnum Trend) are labeled. (See Taylor and others [2009] for names and details regarding other zinc deposits.) Not all the Kipushi-type deposits mentioned in the text appear on this map.

Geology

Gallium occurs in low amounts in a diverse group of geologic environments and is found most commonly in association with deposits of aluminum and zinc (fig. H5), which are its immediate neighbors in the periodic table of elements (fig. H1). The average abundance of gallium in Earth's crust is generally less than 19 parts per million (ppm) (table H2). Because of the rarity of gallium in most geologic environments, minerals containing gallium as an essential structural component are also rare (table H3). Because gallium occurs as a minor or trace element in many minerals, there are a large number of rock types and tectonic settings for mineral deposits that are known to contain gallium in potentially extractable amounts (table H4). At the present time, the majority of the world's supply of newly mined gallium metal comes from bauxite and sediment-hosted lead-zinc deposits (fig. H4). Gallium is currently derived as a byproduct of the processing of bauxite ore for aluminum, with lesser amounts produced from residues resulting from the processing of sphalerite ore for zinc.

Geochemistry

Gallium is a soft, silvery post-transition metal with an atomic number of 31 (table H1; fig. H1) that is very much like aluminum in its chemical properties. The chemical similarities between gallium and aluminum, which include a trivalent oxidation state, a similar atomic radius, tetrahedral or octahedral coordination in minerals, and amphoterism (that is, they can act as both acid and base in reactions), result in their generally synchronous geochemical behavior. Gallium is found primarily in the trivalent oxidation state; mixed-oxidation state compounds containing both Ga^{1+} and Ga^{3+} (ionic radius of about 0.62 angstrom [Å]) occur but are not common (Eagleson, 1994, p. 438). In compounds, gallium exhibits a chemical similarity to Al^{3+} (ionic radius of about 0.54 Å), Fe^{3+} (ionic radius of about 0.69 Å) and Zn^{2+} (ionic radius of about 0.72 Å) (Shannon, 1976) and can substitute for these elements in the common rock-forming minerals (Burton and Culkin, 1978). Other elements typically found in geochemical association with gallium include cadmium, indium, germanium, silicon, and tin (fig. H1). Under certain geochemical conditions, these elements can be separated in near-surface environments—for example, by changes in pH or redox conditions—because their acid/base and electronic properties are sufficiently different (table H1).

The aqueous geochemistry of gallium was studied by Wood and Samson (2006, and references therein) based on a number of earlier works. Trivalent gallium is also the most common oxidation state of gallium metal in aqueous solution and, owing to the high charge, the hydrated ions of gallium are Pearson hard acids (Pearson, 1963), which favor the formation of complexes with hard ligands, such as fluoride, hydroxide, phosphate, and sulfate. In aqueous solutions, gallium is predicted to occur mainly in fluoride and hydroxide complexes (Wood and Samson, 2006). Solubility products of most solid phases containing gallium are generally not available; however, the limited available solubility data constrain the maximum concentrations of gallium to be expected in aqueous fluids to the subparts-per-million to subparts-per-billion (or micrograms per liter) range (Wood and Samson, 2006), and this is evident in the values seen for hydrothermal fluids, river waters, and seawater (table H2). The hydrolysis of GaOOH(s) (solid gallium oxyhydroxide) occurs at low pH, and its speciation is strongly dominated by $Ga(OH)_4^-$ in the pH range of natural solutions at 25 °C. At increasing temperature, the amount of $Ga(OH)_2^+$ and $Ga(OH)_3°$ becomes significant, although at 300 °C, $Ga(OH)_4^-$ remains the predominant species. A comparison of the geochemical behavior of gallium and aluminum in natural fluids indicates that $Ga(OH)_4^-$ exhibits a chemical behavior very similar to that of $Al(OH)_4^-$ (Wood and Samson, 2006). The low solubility of α-GaOOH(s) (in the absence of fluoride or strong organic ligands at low temperatures) is consistent with the immobility of gallium relative to most other elements, except aluminum, during weathering and alteration processes. This immobility leads to the accumulation of gallium in some bauxites and kaolins, and in the high-alumina hydrothermal alteration halos that form around many mineral deposits (for example, epithermal, porphyry, and volcanogenic deposits).

Figure H5. (page H7) Cross sections showing the general geologic environments for the types of mineral deposits with which gallium is most commonly associated and from which gallium is typically extracted. *A*, Karst bauxite deposits, which form by deep weathering and transport of material in carbonate rock-dominated sequences; unlabeled patterns show detritus. *B*, Lateritic bauxite deposits, which form mainly by deep weathering of material in silicate rock-dominated sequences. *A* and *B* modified from Retallack (2010). *C*, Sediment-hosted lead-zinc deposits, which form in passive margin environments. *D*, Clastic-dominated-type lead-zinc deposits, which may form by brine reflux in shales and deep-water carbonates. *E*, Mississippi Valley-type lead-zinc deposits, which form by replacement in platform carbonate sequences. *C*, *D*, and *E* modified from Kelley and others (1995); Bradley and Leach (2003); Leach, Sangster, and others (2005); and Leach, Taylor, and others (2010).

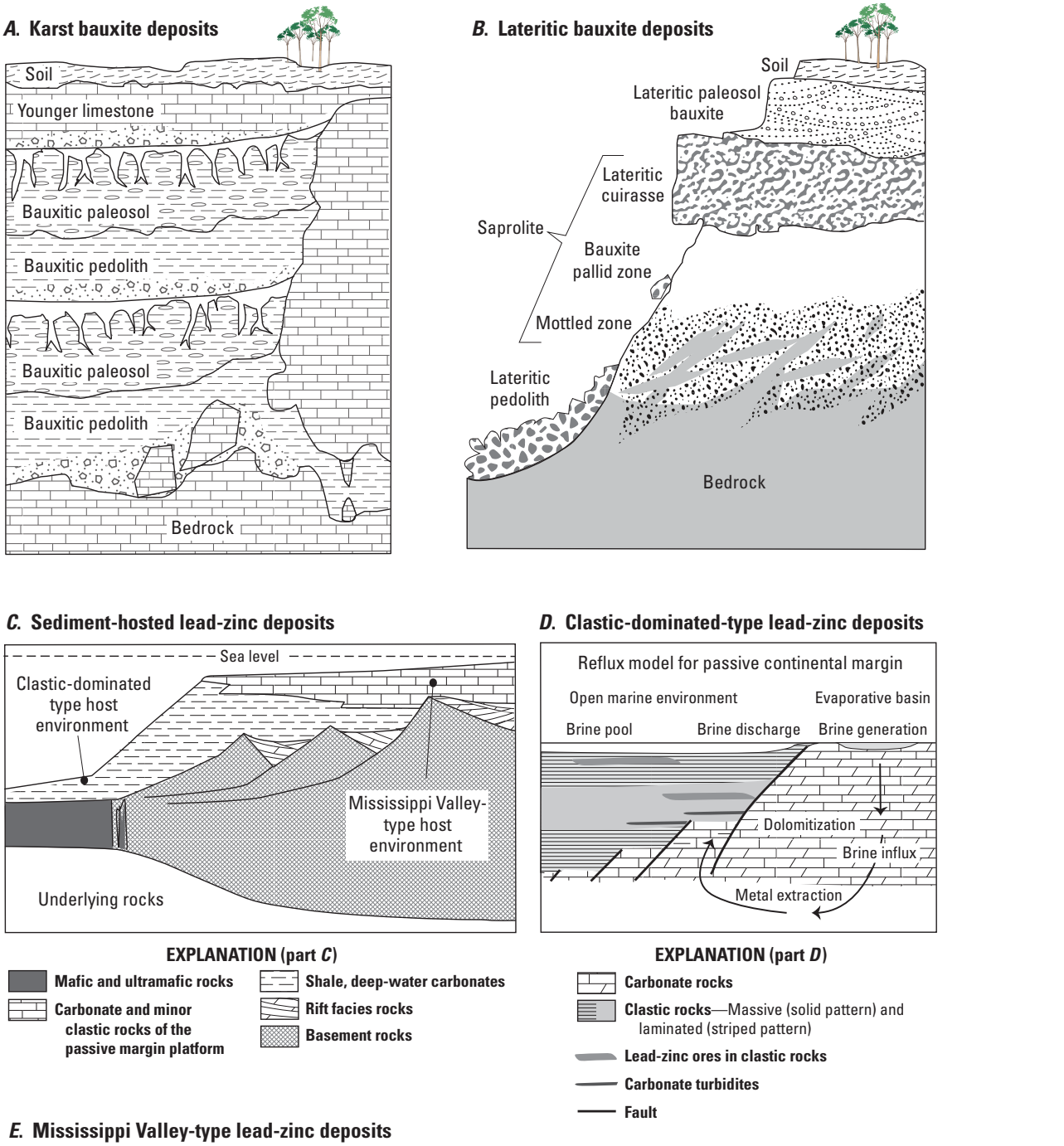

ALL FIGURES NOT TO SCALE

Table H1. Selected properties of gallium, a Group 13 post-transition metal.

[Sources: Instytutu Problem Materialoznavstva (1968) and Lide (2005, p. 14–39). Å, angstrom; °C, degree Celsius; cm, centimeter; eV, electron-volt; g/cm^3, gram per cubic centimeter; GPa, gigapascal; J/mol-K, joule per mole kelvin; K, kelvin; kJ/mol, kilojoule per mole; nΩ-m, nano ohm-meter; µm/m-K, micrometer per meter kelvin; W/m-K, watt per meter kelvin]

Property	Description
Symbol	Ga
Atomic number	31
Atomic weight	69.723
Isotopes	24 radioisotopes; ^{69}Ga, ^{71}Ga are stable isotopes; ^{67}Ga has a half-life of about 3.3 days
Density at 293 K (g/cm^3)	5.91
Melting point (°C)	29.7646
Boiling point (°C)	2,204
Heat of fusion (kJ/mol)	5.59
Heat of vaporization (kJ/mol)	254
Molar heat capacity (J/mol-K)	25.86
Hardness (Mohs scale)	1.5
Brinell hardness (GPa)	0.06
Electrical resistivity at 20 °C (nΩ-m)	270
Thermal conductivity (W/m-K)	40.6
Thermal expansion at 25 °C (µm/m-K)	18
Young's modulus (GPa)	9.8
Crystal structure	Orthorhombic
Magnetic ordering	Diamagnetic
Electron configuration	[Ar] $4s^2 3d^{10} 4p^1$
Ionic radius (Å)	0.62
First ionization potential (eV)	5.999
Second ionization potential (eV)	20.51
Third ionization potential (eV)	30.71
Common valance states	Primarily +3, also +2, +1

Gallium is the 34th most abundant element found in Earth's crust (Emsley, 2001), and it is widely distributed in low amounts in many rock types (table H2). The average values for gallium in igneous rocks vary considerably, from a low of about 5 ppm gallium or less in ultramafic rocks to a range of 10 to 22 ppm for most mafic to intermediate rocks, and to about 16 to 35 ppm gallium for granitic rocks (Burton and Culkin, 1978). Alkaline rocks, particularly nepheline syenites, granites, and related pegmatites, have generally higher ranges, from 20 to 70 ppm gallium (Burton and Culkin, 1978). Values of gallium in shale, sandstone, and carbonates are 19 ppm, 12 ppm, and 4 ppm, respectively (Mielke, 1979), and gallium in loess averages about 14 ppm (McLennan and Murray, 1999).

Gallium contents of rocks may be increased by greisenization, albitization, hydrothermal alteration, and weathering processes, including saprolitization and lateritization. In general, the bulk content of gallium in a given rock type corresponds to the composition and bulk content of feldspar and mica in the rock. Alteration processes that selectively remove mobile elements from aluminosilicate minerals result in relative increases in the concentrations of gallium, aluminum, and other less mobile elements in all rock types. The chalcophile behavior of gallium contributes to its concentration in sulfide ores, which can contain hundreds of parts per million gallium (Burton and Culkin, 1978). In hydrothermal systems related to sulfide mineralization and in residual deposits formed by surficial weathering, the lithophile and chalcophile tendencies of gallium work in opposition in terms of enrichment, as sulfide and aluminosilicate minerals compete for gallium.

The value of the ratio of aluminum to gallium (the Al:Ga ratio) has been used as an indicator of gallium enrichment because it is thought to be relatively constant in most types of crustal rocks (Burton and Culkin, 1978). The value of the Al:Ga ratio in various common rock types can range from 5,000 to 40,000. It is lower, in the range of 1,000 to 10,000, in alkaline igneous rocks and in sedimentary rocks produced by intense weathering (Burton and Culkin, 1978; Tervek and Fay, 1986). Rytuba and others (2003) evaluated the geochemical behavior of gallium in igneous rocks using the worldwide GEOROC (Geochemistry of Rocks of the Oceans and Continents) database (Max Planck Institute, 2002). They found that volcanic rocks from convergent-margin environments with about 8 to 30 ppm gallium had values of Al:Ga that increased from about 3,000 to 8,000 with increasing aluminum content. They concluded that gallium is not enriched by petrologic processes in more evolved silicic volcanic rocks, such as peralkaline rocks, because the Al:Ga ratio did not correlate with increasing quartz (SiO_2) content or alkalinity. A comparison of the data for volcanic rocks worldwide, hydrothermally altered rocks of the McDermitt caldera near the McDermitt Mine in Humboldt County, Nevada (from Rytuba and others, 2003), and globally distributed bauxite deposits shows that gallium concentration is higher in rocks that have lower ratios of Al:Ga owing to hydrothermal alteration and (or) intense weathering (fig. H6). Because the Al:Ga ratio can be quite variable in natural waters (table H2) owing to differences in the mobility of gallium and aluminum in aqueous solutions, the Al:Ga ratio has been used effectively to model the behavior of trace metals as a result of surficial weathering processes (Hieronymus and others, 1990; Shiller and Frilot, 1996) and in ocean waters (Orians and Bruland, 1988; Shiller, 1998) and river waters (Shiller, 1998; Shiller and Frilot, 1996).

Table H2. Gallium concentrations in rocks, ore, coal, soils, and natural waters.

[FOREGS, Forum of European Geological Surveys, now EuroGeoSurveys; Ga, gallium; ICP-MS, inductively coupled plasma-mass spectrometry; XRF, X-ray fluorescence. Units of measure: cm, centimeter; m, meter; mm, millimeter; ppb, part per billion; ppm, part per million; µg/L, microgram per liter; µm, micrometer. —, no data]

Environment and (or) location	Gallium concentration (value or range)		Unit	Type	Notes	Reference(s)
	Typical	Average				
Rocks						
Upper continental crust	—	17, 17.5	ppm	Continental crust	Average	Taylor and McLennan (1995); Rudnick and Gao (2003)
Bulk continental crust	—	18	ppm	Continental crust	Average	Taylor and McLennan (1995)
Lower continental crust	—	18	ppm	Continental crust	Average	Taylor and McLennan (1995)
Volcanic rocks	—	About 8 to 30	ppm	Convergent margins	2,929 analyses	Rytuba and others (2003)
High-sulfidation epithermal	—	Up to 320	ppm	Alteration	None	Melfos and Voudouris (2012)
High-sulfidation epithermal	<9 to 38		ppm	Alteration	None	Khashgerel and others (2008)
All types	8 to 812	41	ppm	Bauxite	None	Schulte and Foley (2014)
Arkansas (lateritic bauxite)	—	86	ppm	Bauxite	None	Burton and Culkin (1978)
Bosnia	—	46	ppm	Bauxite	None	Schulte and Foley (2014)
France	—	63	ppm	Bauxite	None	Schulte and Foley (2014)
India	5 to 122	60	ppm	Bauxite	None	Burton and Culkin (1978)
Karst	10 to 812	41	ppm	Bauxite	None	Schulte and Foley (2014)
Lateritic	8 to 136	56	ppm	Bauxite	None	Schulte and Foley (2014)
Malaysia	22 to 47	33	ppm	Bauxite	None	Burton and Culkin (1978)
Russia	10 to 170	54	ppm	Bauxite	None	Burton and Culkin (1978)
Turkey	—	68	ppm	Bauxite	None	Schulte and Foley (2014)
Indiana—Danville member	1.7 to 8.9	5.06	ppm	Coal	Pennsylvanian	Mastalerz and Drobniak (2012)
Indiana—Springfield member	1.4 to 12.3	3.39	ppm	Coal	Pennsylvanian	Mastalerz and Drobniak (2012)
USGS COALQUAL database	About 3 to 7	—	ppm	Selected domestic coal-bearing regions, averages	Averages	Finkelman (1993)
General	<6 to 66		ppm	Kaolin	None	Hieronymus and others (1990)
Georgia	27 to 100	—	ppm	Kaolin	None	This study; Bárdossy (1982); Bárdossy and Aleva (1990)
Haile kaolin deposit, South Carolina	<6 to 31	19	ppm	Kaolin	None	This study
Malaysia	20 to 25	23	ppm	Kaolin	None	Burton and Culkin (1978)
Geothermal fields	8 to 144	—	ppm	Muds and sinter	None	Crump (1994)

Table H2. Gallium concentrations in rocks, ore, coal, soils, and natural waters.—Continued

[FOREGS, Forum of European Geological Surveys, now EuroGeoSurveys; Ga, gallium; ICP-MS, inductively coupled plasma-mass spectrometry; XRF, X-ray fluorescence. Units of measure: cm, centimeter; m, meter; mm, millimeter; ppb, part per billion; ppm, part per million; µg/L, microgram per liter; µm, micrometer. —, no data]

Environment and (or) location	Gallium concentration (value or range)		Unit	Type	Notes	Reference(s)
	Typical	Average				
Rocks—Continued						
Alkaline	—	About 20 to 70	ppm	Rock	None	Burton and Culkin (1978)
Carbonate rock	—	4	ppm	Rock	Average	Mielke (1979)
Granitic	—	About 16 to 35	ppm	Rock	None	Burton and Culkin (1978)
Loess	—	14	ppm	Rock	Average	McLennan and Murray (1999)
Mafic to intermediate	—	About 10 to 22	ppm	Rock	None	Burton and Culkin (1978)
Peralkaline	—	About 28 to 39	ppm	Rock	None	MacDonald and Bailey (1973)
Shale	—	19	ppm	Rock	Average	Mielke (1979)
Sandstone	—	12	ppm	Rock	Average	Mielke (1979)
Ultramafic	—	About 5	ppm	Rock	None	Burton and Culkin (1978)
Apex Mine, Utah	320 to 1,480	—	ppm	Sulfide	None	Bernstein (1986)
Ruby Creek Mine, Alaska	—	<<1	ppm	Sulfide	None	Bernstein and Cox (1986)
Cadmium-lead-zinc ore, general	<1 to 1,600	60	ppm	Sulfide	None	Schulte and Foley (2014)
Kipushi ore, general	<1 to 2,500	10s to 100s	ppm	Sulfide	None	Schulte and Foley (2014)
Mississippi Valley-type ore, general	<1 to 500	57	ppm	Sulfide	None	Schulte and Foley (2014)
Sulfide ore, bulk	20 to 1,000	100?	ppm	Sulfide	None	Burton and Culkin (1978)
Callahan Mine, Maine	—	25	ppm	Volcanogenic massive sulfide, bulk sulfide	None	Ayuso and others (2013)
Red Dog Mine, Alaska	—	26	ppm	Clastic-dominated, ore concentrate	None	Alaska Department of Environmental Conservation (2005)
Soils						
World	—	17	ppm	Soil, bulk	None	Koljonen (1992)
Western United States	—	16	ppm	Soil	Mean for 20 cm depth	Shacklette and Boerngen (1984)
Eastern United States	—	9.3	ppm	Soil	Mean for 20 cm depth	Shacklette and Boerngen (1984)
Poland	—	100±5	ppm	Soil	Agricultural	Połedniok and others (2012)
Poland	—	219±5	ppm	Soil	Agricultural	Połedniok and others (2012)
Poland	—	38±4	ppm	Soil	Agricultural	Połedniok and others (2012)
Poland	—	93±7	ppm	Soil, proximal to a former Zn-Pb mine	Proximal to a former Zn-Pb mine	Połedniok and others (2012)
Poland	—	268±19	ppm	Soil, proximal to Zn-Pb ore and a bauxite mine	Proximal to Zn-Pb ore and a bauxite mine	Połedniok and others (2012)
Sweden	—	7 to 13	ppm	Soil developed on quartzite and gneiss	Profile range	Tyler (2004)

Table H2. Gallium concentrations in rocks, ore, coal, soils, and natural waters.—Continued

[FOREGS, Forum of European Geological Surveys, now EuroGeoSurveys; Ga, gallium; ICP-MS, inductively coupled plasma-mass spectrometry; XRF, X-ray fluorescence. Units of measure: cm, centimeter; m, meter; mm, millimeter; ppb, part per billion; ppm, part per million; µg/L, microgram per liter; µm, micrometer. —, no data]

Environment and (or) location	Gallium concentration (value or range)		Unit	Type	Notes	Reference(s)
	Typical	Average				
Soils—Continued						
FOREGS samples, median concentration	—	0.9	ppm	Humus, median concentration	<2.0 mm fraction, n=367, Total (ICP-MS)	Salminen (2015)
FOREGS samples, median concentration	—	13.5	ppm	Topsoil	<2.0 mm fraction, n=843, Total (ICP-MS)	Salminen (2015)
FOREGS samples, median concentration	—	13.8	ppm	Subsoil	<2.0 mm fraction, n=790, Total (ICP-MS)	Salminen (2015)
Waters						
Atlantic Ocean	—	0.0003 to 0.004	µg/L	Seawater	Dissolved and colloidal (<0.4 µm); surface to 5,000 m deep	Shiller (1998)
African rivers	—	0.02 to 0.11	µg/L	River	Dissolved load (<0.2 µm)	Gaillardet and others (2003)
North American rivers	—	0.001 to 0.012	µg/L	River	Dissolved load (<0.2 µm)	Gaillardet and others (2003)
South American rivers	—	0.003 to 0.12	µg/L	River	Dissolved load (<0.2 µm)	Gaillardet and others (2003)
California streams	—	0.0001 to 0.006	µg/L	River	Dissolved and colloidal load (<0.4 µm)	Shiller and Frilot (1996)
Idel River	—	0.009	µg/L	River	Dissolved load (<0.2 µm)	Gaillardet and others (2003)
Japan	—	2.5	ppb	Geothermal	None	Uzumasa and Nasu (1960)
Wairakei, New Zealand	—	About 0.2	ppb	Geothermal	None	Goguel (1988)
Broadlands, New Zealand,	—	About 0.2	ppb	Geothermal	None	Goguel (1988)
Bath, United Kingdom	—	0.63	ppb	Geothermal	None	Riley (1961)
Taiwan	—	0.01 to >10.00	µg/L	Groundwater	None	Chen (2006)
World rivers	18.1	—	ppm	Suspended sediment	Average	Viers and others (2009)
FOREGS samples, median concentration	—	0.011	µg/L	Water	Filtered <0.45 micrometer fraction	Salminen (2015)
FOREGS samples, median concentration	—	12.0	ppm	Stream sediment	<2.0 mm fraction, n=852, Total (XRF)	Salminen (2015)
FOREGS samples, median concentration	—	11.0	ppm	Flood plain sediment	<2.0 mm fraction, n=747, Total (XRF)	Salminen, 2015

Mineralogy

Gallium is an essential structural component of only a few minerals that form in nature. Gallium is dispersed, however, in low amounts in many minerals and rocks, where it substitutes for elements of similar size and charge (table H3). Because gallium minerals are too rare in nature to serve as a primary source of the element or its compounds, most gallium is produced from minerals containing less than 100 ppm gallium (table H3), where the gallium may occur as inclusions, as stoichiometric or nonstoichiometric substitutions, or as adsorbed ions or molecules.

Four gallium-rich minerals have been recognized (approved) by the International Mineralogical Association, Commission on New Minerals, Nomenclature and Classification (table H3). These include the sulfide gallite, which has about 35 weight percent gallium; gallobeudantite, which is an alunite of variable gallium content; and the hydroxide minerals sohngeite and tsumgallite, both of which contain about 60 weight percent gallium. These minerals have been identified in association with carbonate-hosted copper-lead-zinc deposits at the Tsumeb Mine in the Oshikoto Region, Namibia (Frimmel and others, 1996, and references therein). Gallite occurs as a primary sulfide mineral and is essentially a common copper sulfide, chalcopyrite ($CuFeS_2$), in which gallium replaces iron in the crystal structure. Typical occurrences of gallite are as inclusions in sphalerite (ZnS). Because gallite has a chalcopyrite structure, it may occur as either epitaxial overgrowths or inclusions as "chalcopyrite disease" (Barton and Bethke, 1987) in sphalerite. Gallobeudantite, sohngeite, and tsumgallite are supergene minerals resulting from surficial oxidation of other gallium-bearing minerals. Gallium also substitutes in many minerals, including silicates, sulfides, and hydroxides, in concentrations ranging from parts per million to weight percent (table H3). For example, significant amounts occur in krieselite (about 20 weight percent gallium), which is the germanium analog of topaz, and in gallium-rich plumbogummite, where it may fill one-third of the aluminum sites (about 25 weight percent gallium). Major rock-forming minerals, however, contain significantly less than 1 percent gallium, and most minerals have less than 100 ppm gallium. Feldspars and micas are the dominant host minerals for gallium in most igneous and sedimentary rocks. For example, gallium has been reported at relatively

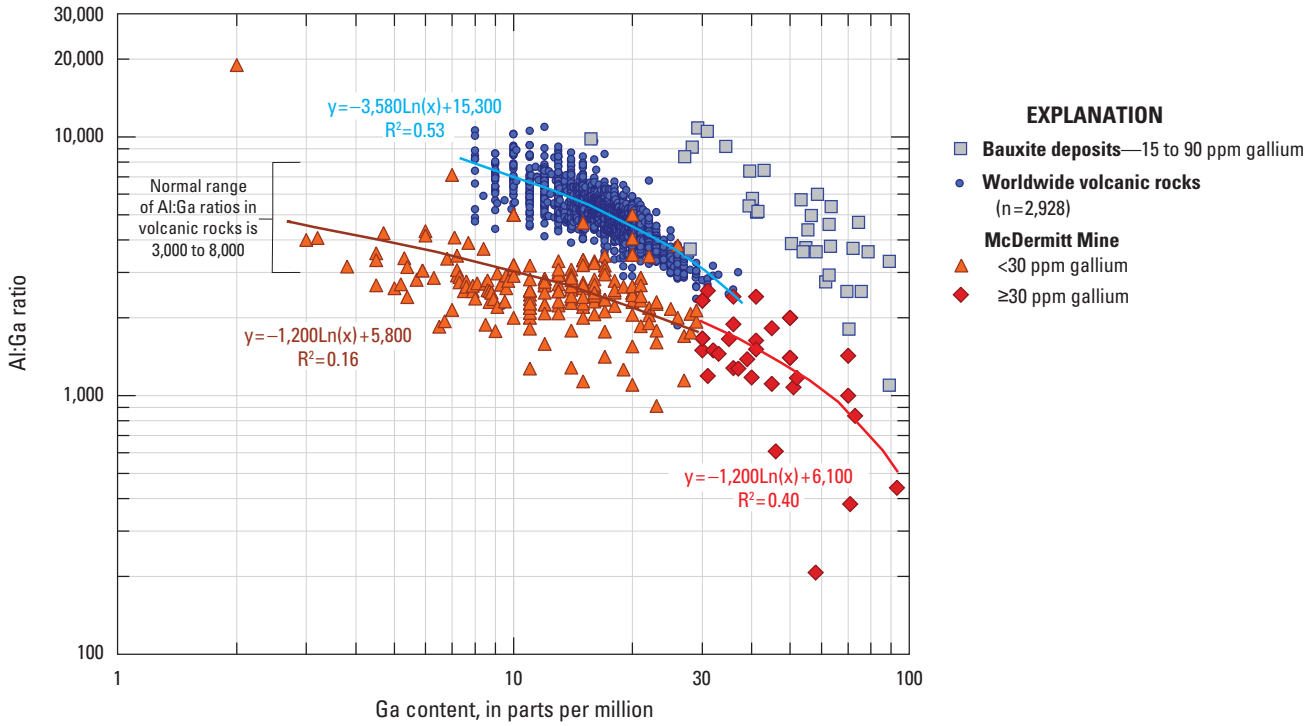

Figure H6. Plot of the ratio of aluminum to gallium (Al:Ga, log scale) versus gallium content (in parts per million [ppm], log scale) for bauxite deposits, volcanic rocks, and hydrothermally altered rocks of the McDermitt caldera, Nevada. Results from the McDermitt Mine, Nev., are included for comparison; see text for details. Equations define slope of lines drawn through datasets for comparison; R^2 value is a measure of goodness of the fit of the line to the data. Modified from Rytuba and others (2003) with the addition of data for various globally distributed bauxite deposits from Schulte and Foley (2014).

Table H3. Selected gallium-bearing minerals—Formula, content, and occurrence.

[Compiled from Burton and Culkin (1978), Bernstein (1986), Dutrizac and others (1986), Tervek and Fay (1986), Frimmel and others (1996), Schlüter and others (2003), Ye and others (2011), and Schulte and Foley (2014). b.d.l., below detection limit; ppm, part per million; ~, approximately. Elements: Al, aluminum; Cu, copper; Fe, iron; Ga, gallium; Pb, lead; Zn, zinc]

Mineral name	Chemical formula	Ga content	Group	Deposit model, occurrence type
Minerals with essential gallium[1] (weight percent)				
Gallite	$CuGaS_2$	35.32	Sulfide	Carbonate-hosted Cu-Pb-Zn; Pb-Zn-Cu Tsumeb Mine in Namibia
Gallobeudantite	$PbGa_3[(AsO_4),(SO_4)]_2(OH)_6$	14.55, variable	Alunite	Carbonate-hosted Cu-Pb-Zn; supergene, Tsumeb Mine in Namibia
Sohngeite	$Ga(OH)_3$	57.74	Hydroxide	Carbonate-hosted Cu-Pb-Zn; supergene, Tsumeb Mine in Namibia.
Tsumgallite	GaO(OH)	59.93	Hydroxide	Carbonate-hosted Cu-Pb-Zn; supergene, Tsumeb Mine in Namibia
Minerals with nonessential gallium				
Krieselite	$(Al,Ga)_2(GeO_4)(OH)_2$	20.3 weight percent	Topaz group, germanate	Ge analog of topaz
Sphalerite	ZnS	b.d.l. to 2,500 ppm	Sulfide	Volcanogenic massive sulfide, sedimentary exhalative, and Mississippi Valley-type base-metal deposits
Eyselite	$FeGe_3O_7(OH)$	6,900 ppm	Hydroxide	Carbonate-hosted Cu-Pb-Zn; Pb-Zn-Cu Tsumeb Mine in Namibia
Ovamboite	$Cu_{20}(Fe,Cu,Zn)_6W_2Ge_6S_{32}$	4,600 ppm	Sulfide, germanite group	Massive sulfide base-metal ores
Calvertite	$Cu_5Ge_{0.5}S_4$	3,500 ppm	Sulfide	Carbonate-hosted Cu-Pb-Zn; Pb-Zn-Cu Tsumeb Mine in Namibia
Ferrohogbomite-2N2S	$(Fe,Zn,Mg,Al)_6Al_{14}(Ti,Fe)_2O_{30}(OH)_2$	1,600 ppm	Oxide	High grade Fe-oxide deposits
Maikainite	$Cu_{20}(Fe,Cu)_6Mo_2Ge_6S_{32}$	1,500 ppm	Sulfide, germanite group	Volcanogenic massive sulfide, sedimentary exhalative, and Mississippi Valley-type base-metal deposits. (1) Maikain deposit, Kazakhstan, and (2) Tsumeb deposit, Namibia
Plumbogummite, Ga-rich	$PbH(Al,Ga)_3(PO_4)_2(OH)_6$	~25 weight percent	Crandallite subgroup, alunite supergroup	Carbonate-hosted Cu-Pb-Zn; Pb-Zn-Cu Tsumeb Mine in Namibia
Gibbsite	$Al(OH)_3$	About 50 ppm	Oxide, hydroxide	Bauxite-silicate; bauxite-karst
Diaspore	α-AlO(OH)	About 50 ppm	Oxide, hydroxide	Bauxite-silicate; bauxite-karst
Boehmite	γ-AlO(OH)	About 50 ppm	Oxide, hydroxide	Bauxite-silicate; bauxite-karst
Kaolinite	$Al_2Si_2O_5(OH)_4$	About 50 to 200 ppm	Silicate	Kaolins; bauxite-silicate; bauxite-karst
Halloysite	$Al_2Si_2O_5(OH)_4$	About 50 to 200 ppm	Silicate	Kaolins; bauxite-silicate; bauxite-karst
Jarosite	$KFe(SO_4)_2(OH)_6$	0.7 weight percent	Sulfite	Supergene
Limonite	$FeO(OH)•nH_2O$	2 weight percent	Hydroxide	Supergene
Goethite	FeO(OH)	200 ppm	Hydroxide	Supergene
Renierite	$(Cu,Zn)_{11}(Ge,As)_2Fe_4S_{16}$	0.04 to 400 ppm	Sulfide, germanite group	Massive sulfide base-metal ores
Germanite	$Cu_{26}Fe_4Ge_4S_{32}$	0.09 to 900 ppm	Sulfide, germanite group	Massive sulfide base-metal ores
Feldspar group	$NaAlSi_3O_8$, $CaAl_2Si_2O_8$, $KAlSi_3O_8$	b.d.l. to 100 ppm, rarely up to 4,000 ppm	Silicate	Felsic igneous rocks

[1]Approved by the International Mineralogical Association, Commission on New Minerals, Nomenclature and Classification.

high concentrations (0.05 weight percent) in feldspars from the Nechalacho layered nepheline-aegirine syenite suite at Thor Lake in the Northwest Territories, Canada (Tervek and Fay, 1986); however, most feldspar contains much less than 200 ppm gallium (table H3). Gallium is retained in clay minerals, such as kaolinite and smectite, and in aluminum hydroxide minerals during weathering, which accounts for the higher gallium contents in many clay-bearing rocks and bauxites (table H2). At the present time, gallium is derived mainly from aluminum hydroxide minerals, including boehmite, diaspore, and gibbsite ($Al(OH)_3$), which form in deeply weathered deposits of bauxite (fig. H7*A*) (Dutrizac and others, 1986; Bernstein and Waychunas, 1987; Moskalyk, 2003). Significant amounts of gallium are also produced from zinc sulfide deposits where sphalerite (fig. H7*B*) is the main carrier (Moskalyk, 2003). Gallium (and germanium) can also be enriched in other sulfide minerals, such as bornite, enargite, galena, and luzonite (Hörmann, 1978). Weathering of gallium-bearing sulfide minerals can lead to gallium-enriched sulfate and hydroxide minerals, and in oxidized environments, gallium commonly occurs in plumbojarosite and hydrogoethite (Burton and Culkin, 1978). At the Apex Mine in Summit County, Utah, jarosite (a potassium-iron-sulfate mineral) reportedly contains concentrations of up to 1 weight percent gallium (Bernstein, 1986).

Gibbsite-Diaspore-Boehmite

Gibbsite forms in weathering environments by a series of reactions generated during the hydrolysis of feldspar and other aluminosilicate minerals in rocks undergoing saprolitization (Foley and Ayuso, 2013, and references therein). The proportion of gibbsite-diaspore-boehmite increases at the expense of kaolinite in more intensely weathered rocks, such as bauxites and laterites (Soler and Lasaga, 1996). In these environments, as a result of burial diagenesis or low-grade regional metamorphism, gibbsite transforms to boehmite (γ-AlO(OH)) by dehydration, and turns into diaspore (α-AlO(OH)) after compaction. Gallium in these minerals may be found as substitutions for trivalent aluminum or it may form as a separate phase (table H3). Sohngeite, which is the gallium analog of gibbsite, has a similar stability, and it transforms readily into tsumgallite (GaO(OH)) in aqueous solution (table H3). The unit cell parameters of tsumgallite mostly resemble diaspore compared with gibbsite or boehmite (Schlüter and others, 2003). Gallium hydroxide minerals rarely form as discrete phases; rather, they generally occur in supergene parts of carbonate-hosted polymetallic replacement deposits, such as at the Tsumeb Mine in Namibia (Frimmel and others, 1996). Diaspore and tsumgallite are isostructural, have similar crystal chemical characteristics, and are the most

Figure H7. Photographs showing samples of *A*, bauxite ore, and *B*, sphalerite ore, which are the primary mineralogical sources of gallium. The three samples of bauxite are from U.S. Geological Survey (USGS) collections and the powdered bauxite ore sample was provided by E.L. Bray, USGS. The sphalerite ore is from the Creede district, San Juan County, Colorado.

stable hydroxides of aluminum and gallium, respectively. Thus, gallium, in the form of GaO(OH), is more likely to be enriched in diaspore than in the other aluminum hydroxides.

Sphalerite

Sphalerite (fig. H7*B*) is an important source of gallium in spite of the generally low concentrations in natural samples (table H3) because it is abundant in a wide variety of mineral deposits (table H4). Gallium enrichment in sphalerite under hydrothermal conditions results from its weak chalcophile behavior, which is similar to that of zinc. Gallium is thought to be incorporated in sphalerite by a coupled substitution of two Zn for Ga plus either Ag, Cu, Ge, In, or Sn to maintain a balanced charge (Johan and others, 1983; Johan, 1988; Cook and others, 2009). The highest known concentrations of gallium in sphalerite (2.1 to 3.7 weight percent gallium occur in sulfide nodules in the Qingzhen (EH3) chondrite (Rambaldi and others, 1986), which is a range that matches experimental determinations (Krämer and others, 1987; Ueno and Scott, 2002). Sphalerite from gallium-rich low temperature carbonate-hosted lead-zinc deposits of Namibia (Khusib Spring Mine in the Otjozondjupa Region and the Tsumeb Mine) show a range of from hundreds to more than 3,000 ppm gallium (Melcher and others, 2006). In general, however, concentrations in most sphalerites rarely exceed 100 ppm gallium. For example, sphalerite from clastic-dominated lead-zinc deposits of the Red Dog Mine in the Northwest Arctic Borough of Alaska contains an average of 26 ppm gallium (Alaska Department of Environmental Conservation, 2005), whereas zinc ores from U.S. Mississippi Valley-type deposits average about 50 ppm gallium (Moskalyk, 2003). Gallium contents can vary widely in volcanogenic massive sulfide deposits, even within a single district or within individual sphalerite grains from a deposit. For example, some individual deposits within the Bonnifield mining district in Alaska (such as the Anderson Mountain deposit in Denali Borough and the Fosters Creek zone) can contain anywhere from 20 to 275 ppm gallium in sphalerite, whereas others (the West Tundra Flats deposit in Southeast Fairbanks Borough) have less than 1 ppm gallium in sphalerite (Foley and others, 2008; Dusel-Bacon and others, 2011; Dusel-Bacon and others, 2012). Sphalerite from the Callahan Mine in Hancock County, Maine (Ayuso and others, 2013), shows a range of from less than 3 ppm to up to 105 ppm gallium in single, 1- to 5-millimeter (mm)-wide crystals (table H3).

Deposit Types

The principal deposit types (table H4) and significant global and domestic deposits (fig. H4) from which gallium metal is currently being obtained are emphasized here; however, other deposit types that have gallium in potentially extractable amounts are included in table H4. Although gallium is found in a diverse group of mineral deposit types, current sources are limited to a small number of deposit types because gallium is produced mainly as a byproduct. More than 80 percent of the world's refined gallium is obtained from bauxite deposits (Jaskula, 2013b). The balance is derived from operations that collect zinc residues from a variety of zinc deposit types; the residues are combined prior to the gallium extraction cycle. Among zinc deposits, gallium concentrations tend to be high in carbonate-hosted replacement deposits and Mississippi Valley-type deposits, and variably enriched in clastic-dominated systems and volcanogenic massive sulfide deposits, whereas skarns are universally low in gallium (Cook and others, 2009). Gallium and other metals produced from zinc-refining residues are derived largely from such deposits as the Red Dog zinc mine in Alaska (Tervek and Fay, 1986). Other sources include volcanogenic massive sulfide deposits; for example, the Tizapa Mine in Mexico (Dowa Holdings Co., Ltd., 2013). Carbonate-hosted lead-zinc deposits of the Kipushi-type—for example, the Apex Mine in Utah—have the potential to produce gallium (and germanium) as a primary product. The two major types of gallium sources—bauxite deposits and sediment-hosted lead-zinc deposits—are described below.

Bauxite Deposits

Bauxite is mined for a number of products that have commercial application in abrasive, cement, chemical, metallurgical, and refractory industries. Approximately 70 to 80 percent of the world's dry bauxite production is processed into aluminum metal (Freyssinet and others, 2005), and these are the ores from which most gallium metal is currently derived. Bauxite is a rock that consists mostly of fine-grained aluminum minerals, notably boehmite, diaspore, and gibbsite, in mixtures with lesser amounts of iron oxides, typically goethite and hematite, kaolinite, and small amounts of anatase (Bárdossy and Aleva, 1990). Some bauxites form as accumulations of clayey remnants within paleokarst disconformities in limestone sequences; these are referred to as karst bauxites (fig. H5*A*). Karst bauxite is typically black to gray in color because of the presence of admixed organic matter and, in some instances, minerals that form in chemically reduced environments, such as pyrite (Bárdossy, 1982). Another type of bauxite, lateritic bauxite, occurs in parts of thick altered profiles formed by lateritization of aluminosilicate rocks (fig. H5*B*) (Retallack, 2010). Lateritization is a complex integration of surficial biological, chemical, and physical processes that result in thick sequences of intensely weathered saprolite and soil. Laterites are a form of ferricrete that can occur as horizons within a soil profile. By definition, periods of lateritization record exceptionally intense, regionally widespread weathering under tropical temperature regimes with ample water (Bárdossy and Aleva, 1990); thus, lateritic bauxites occur in thick profiles formed by deep tropical weathering. A combination of climate, tectonics, geomorphology, and hydrogeological factors are required to produce deposits that make up productive bauxite ore districts and provinces (fig. H4; Bogatyrev, Zhukov, and Tsekhovsky, 2009).

Table H4. Significant global and domestic deposit types from which gallium is obtained or is potentially extractable.

[VMS, volcanogenic massive sulfide; Elements: Au, gold; Ag, silver; Al, aluminum; As, arsenic; Cd, cadmium; Co, cobalt; Cu, copper; Ga, gallium; Ge, germanium; Hg, mercury; In, indium; Pb, lead; Zn, zinc]

Petrologic association		Principal commodity (byproduct)	Tectonic/deposit character	Description		Primary references
				Example deposits/occurrences	Gallium host mineralogy	
Volcanic-hosted, hydrothermal	Hydrothermal, hot springs	Au	Active epithermal gold-depositing environments	Taupo Volcanic Zone, Rotokawa geothermal system, New Zealand	Muds and sinters of geothermal fields; alunite, other aluminous phosphate minerals	Crump (1994)
	High-sulfidation epithermal gold	Au	Aluminum-phophate-sulfate minerals occurring in the advanced argillic zone of alteration	Hugo Dummett porphyry copper-gold deposit, Mongolia; Agios Philippos Mine, Kirki, Greece; Lavrion intrusion-related deposit, Plaka deposit, Greece	Aluminosilicate minerals, alunite, other aluminous phosphate minerals, aluminum hydroxide	Khashgerel and others (2008); Melfos and Voudouris (2012)
	Epithermal mercury	Au, Ag, Hg	Tertiary age andesite and rhyolite volcanic flows	Gold Canyon's Cordero Gallium Project, McDermitt, Nevada, United States	Alunite, other aluminous phosphate minerals	Rytuba and others (2003)
	Volcanogenic massive sulfide	Zn, Cu, Pb (Au, Ag)	Submarine volcanoes of backarc basins	Tizapa zinc mine, Mexico; Bonnifield district, Alaska; Bald Mountain, Maine, United States	Sphalerite	Shanks and Thurston (2012); Dusel-Bacon and others (2012)
Sediment-hosted	Clastic-dominated lead-zinc	Zn, Pb, Cu, Ag (Ga, In, Ge)	Clastic-dominated lead-zinc ores, which are hosted in shale, sandstone, siltstone, or mixed clastic rocks, or occur as carbonate replacement, within a clastic-dominated sedimentary rock sequence	Red Dog zinc mine, Howards Pass, Su-Lik, and Anarraaq, Alaska, United States; Sullivan, British Columbia, Canada; Broken Hill, Australia; Balmat-Edwards, New York, United States; Rammelsberg, Meggen, Germany	Sphalerite	Leach, Bradley, and others (2010); Leach, Taylor, and others (2010); Taylor and others (2009)
	Mississippi Valley-type	Pb, Zn, Cu, (Ge, Ag, Ga, As, Cd)	Carbonate-hosted lead-zinc deposits, which are typically found in platform carbonate sequences in passive-margin tectonic settings	Tri-State area in the United States (Southeastern Missouri, Eastern and Central Tennessee, Northern Arkansas); Pine Point, Canada; Polaris, Nanisivik, Alaska, United States; Navan, Ireland	Sphalerite	Leach, Bradley, and others (2010); Leach, Taylor, and others (2010); Taylor and others (2009)
	Carbonate-hosted Cu±Pb±Zn (alt. Tsumeb or Kipushi)	Cu, Pb, Zn (Co, Ge, Ag, Ga, As, Cd)	Carbonate-hosted (karstic) polymetallic deposits found in intracratonic platform and rifted continental margin sedimentary sequences; typically folded and locally faulted; often overlain disconformably by oxidized sandstone-siltstone-shale units. Largest deposits are epigenitic replacements within thick sedimentary sequences	Grinnell and Kanuyak Island, Northwest Territories, Canada; Gortdrum, Ireland; M'Passa, Republic of the Congo; Timna, Israel; Nifty, Australia; portions of the Dongchuan deposits, China; Ruby Creek and Omar deposits, Alaska, United States; Tsumeb and Kombat, Namibia; Kipushi, Democratic Republic of the Congo; Apex Mine, Utah, United States	Sphalerite	Söhnge (1964); Intiomale and Oosterbosch (1974); Bernstein (1986)

Table H4. Significant global and domestic deposit types from which gallium is obtained or is potentially extractable.—Continued

[VMS, volcanogenic massive sulfide; Elements: Au, gold; Ag, silver; Al, aluminum; As, arsenic; Cd, cadmium; Co, cobalt; Cu, copper; Ga, gallium; Ge, germanium; Hg, mercury; In, indium; Pb, lead; Zn, zinc]

Petrologic association		Principal commodity (byproduct)	Tectonic/deposit character	Description		Primary references
				Example deposits/occurrences	Gallium host mineralogy	
Weathering-related	Bauxite, karstic	Al (Ga)	Formed by deep, in situ weathering, transport, and accumulation of intercalated clays or by clay dissolution residues of limestone or other carbonate rocks, karst setting, accumulation of aluminum hydroxide minerals	Europe (France, Croatia, Italy); Jamaica; bauxite mine in Arkansas, United States; China	Gibbsite, diaspore, boehmite	Freyssinet and others (2005); Retallack (2010); Bárdossy (1982), Bogatyrev, Zhukov, and Tsekhovsky (2009)
	Bauxite, lateritic	Al (Ga)	Formed by lateritization of various predominately silicate rocks such as granite, gneiss, basalt, syenite, and shale. Intense mineral hydrolysis resulting in kaolinite dissolution and precipitation of aluminum hydroxide minerals	Major bauxite provinces; mostly in the countries of the tropics (current and paleo): (1) the South American province. includes the Guiana shield (Guyana, French Guiana, Suriname) and the central Brazilian shield; (2) the West African province, includes Guinea, Ivory Coast, Burkina Faso, Sierra Leone, Ghana, and Mali; (3) the Indian province, includes both the western and eastern coasts of India; (4) the South East Asian province, includes Vietnam, Laos, and Cambodia; and (5) the Austalian province. Minor provinces include the southern United States and the southern Ural Mountains (Russia and Kazakhstan)	Gibbsite, diaspore, boehmite	Freyssinet and others (2005); Retallack (2010); Bárdossy and Aleva (1990); Bogatyrev, Zhukov, and Tsekhovsky (2009)
	Supergene, gossan	Ge, Ga	Gossans and other oxidized zones of copper-rich, arsenic-bearing sulfide deposits, particularly those of the carbonate hosted polymetallic Kipushi-type rocks	Apex Mine, Utah, United States; see Carbonate-hosted Cu±Pb±Zn, Kipushi-type	Jarosite, Fe-hydroxide, Ga-hydroxides	Bernstein (1986); Dutrizac and others (1986)
	Coal	Coal (Ga?)	Coal seams and waste products from coal-fired powerplants; gallium is enriched in fly ash, sometimes 6 to 10 times more than in the feed coal	Jungar Coalfield, Inner Mongolia; West Virginia, United States; Canada	Coal, fly ash, kaolinite, boehmite	Finkelman (1993)

The formation of large and superlarge deposits is thought to require more than 10 million years or the superposition of several intense weathering epochs.

Various models for the origin of laterites and lateritic bauxites (for example, McFarlane, 1976; Brimhall and others, 1991; Retallack, 2010) have included both (a) elemental removal by hydrolysis and chemical leaching, and (b) elemental addition by mineral precipitation or fluvial or atmospheric deposition (for example, eolian dust) to explain the chemical compositions and volume and mass losses in bauxites. Bauxites usually form in the pallid soil zone (fig. H5*B*) but can occur in the B or C horizons of exceptionally thick profiles (Retallack, 2010). Lateritic bauxites typically have distinctive pisolitic textures and red colors (fig. H7*A*). Karst bauxites that form by transport and redeposition of lateritic bauxite clays and rubble in paleokarst depressions may retain the laterite characteristics of color and texture (Retallack, 2010). The extreme weathering conditions that contribute to bauxite formation remove virtually all the alkalis and alkaline earths, leaving only the relatively immobile component of the original rock; as a result, paleosols within bauxites and soils that form on bauxite are classified as oxisols (U.S. Natural Resources Conservation Service, Soil Survey Staff, 2000).

Bauxite deposits form in a diverse array of geologic and tectonic environments over a wide range of geologic time (for example, Bárdossy, 1982; Bárdossy and Aleva, 1990; Retallack, 2010). An extensive study of well-characterized and dated bauxites (Retallack, 2010) showed that although the oldest known bauxites formed on the Arabian Shield at about 3,500 mega-annum (Ma, or million years ago), bauxites are most abundant in rocks formed since about 100 Ma owing to better preservation of the rock record (Wilkinson and others, 2009). Bauxites show an uneven distribution through time that is consistent with evidence supporting their correlation with paleoclimatic events of intense weathering, possibly related to greenhouse gas emissions, which lasted for geologic time intervals of less than about 100,000 years (Valeton, 1983; Retallack, 2010). Bauxite formation during these events had an expanded distribution from the Quaternary (between the Tropics of Cancer and Capricorn) to encompass areas near the Arctic and Antarctic Circles (Retallack, 2010). As a consequence, greenhouse gas events of the past, which are shown to have influenced the distribution of aluminum ores (Retallack, 2010), are also associated with gallium ores.

Bauxite, lateritic bauxite, and karst bauxite are rocks that have concentrations of aluminum exceeding about 45 percent by weight, by definition (Valeton, 1972). This reflects a high proportion of hydroxide minerals with aluminum contents on the order of about 60 or more percent alumina by weight. Bauxite generally is defined as rock with 20 percent or less total iron, whereas lateritic bauxite, in addition to a high percentage of aluminum, can have greater than 20 percent total iron, which is generally ferric owing to oxidation unless reducing conditions prevail locally. The limited mobility of aluminum and gallium in near-surface environments accounts for gallium enrichment in bauxite and related materials (soils, kaolins, and ball clays) derived from deep weathering of crustal rocks. Overall, bauxite contains concentrations in the range of 8 to 800 ppm gallium, with most values in the range 40 to 80 ppm gallium (table H2). The world average concentration of gallium in bauxite was initially estimated to be 52 ppm (Burton and Culkin, 1978), and additional data have not changed that value significantly. For example, carbonate-hosted bauxites from central and southern Europe display average concentrations of about 50 ppm gallium (Schroll, 1999); bauxites from Arkansas range from 50 to 100 ppm gallium (average 86 ppm); and bauxite from India has a similar range of 5 to 122 ppm gallium (table H2). High gallium values are reported in bauxite originating from alteration of alkali rocks (for example, nepheline syenite of Russia ranges up to 170 ppm gallium) and in some unusual karst deposits (table H2). In general, however, there appear to be no significant differences in gallium concentrations of karst- or lateritic-type bauxites (Schulte and Foley, 2014).

Sediment-Hosted Lead-Zinc Deposits

Sediment-hosted lead-zinc deposits are historically the most significant sources of zinc, and these deposits are mined throughout the United States and the world (Leach, Bradley, and others, 2010). The largest and most economically important sediment-hosted deposits for zinc production are the clastic-rock-dominated and carbonate-rock-dominated (Mississippi Valley-type) subtypes (Leach, Marsh, and others, 2004; Leach, Bradley, and others, 2010; Leach, Taylor, and others, 2010); these are the main types of sulfide deposits from which gallium metal is obtained at present because they are currently the predominant sources of zinc ore. Carbonate-hosted polymetallic deposits of the Kipushi (or Tsumeb) type are of minor importance for zinc production; however, they are considered separately here because they have high gallium content relative to other deposit types of the sediment-hosted class and are historic gallium producers for the United States. Much of the following discussion is summarized from a number of seminal review studies of sediment-hosted lead-zinc deposits, including Leach and Sangster (1993), Leach, Viets, and others (1995); Leach, Marsh, and others (2005); Leach, Sangster, and others, (2005); Groves and Bierlein (2007); Leach, Bradley, and others (2010); and Leach, Taylor, and others (2010).

Sediment-hosted lead-zinc deposits form in rocks of widely varying geologic age and tectonic environment (figs. H5*C* through H5*E*). In general, these deposits are hosted by large-scale sedimentary systems consisting of a variety of siliciclastic and carbonate rocks and have no direct genetic association with igneous activity. Many deposits in the sediment-hosted class display transitional features, and the distinctions among some of the deposit types are subjective. Most sediment-hosted deposits occur in sedimentary rock sequences that were originally deposited in extensional rift or passive-margin settings. There is an apparent uneven distribution of sediment-hosted deposits through time that is

attributed to their genesis in large-scale sedimentary systems and to continued recycling of the sedimentary rock record within the evolving tectonic and geochemical systems of Earth through geologic time. Tectonic setting, depositional environment, and host-rock lithology influence the mineral chemistry of the contained sulfide minerals, including their trace element characteristics. The ores consist mainly of galena, sphalerite, and generally lesser amounts of iron sulfides, which may be marcasite or pyrite. In addition to lead and zinc, gallium, germanium, and silver can be important constituents; copper is generally quite low, except in the Kipushi-type deposits, but can be economically important in all these deposits. Laminated ore textures and a layered morphology are generally characteristic of clastic-dominated deposits, whereas Mississippi Valley-type deposits generally exhibit abundant evidence for epigenetic and replacement ores. Nonetheless, some clastic-dominated ores show replaced sediments in early or burial diagenetic environments and some Mississippi Valley-type deposits display laminated ore textures.

Clastic-Dominated Lead-Zinc Type

The most definitive characteristic of clastic-dominated deposits as described by Leach, Marsh, and others (2005) is their occurrence in clastic rock-dominated sedimentary sequences formed mainly in passive margins, continental rifts, continental sag basins, and back-arc basins (figs. H5*C* and H5*D*). The orebodies are typically hosted in (in order of predominance) shale, sandstone, siltstone, carbonate, or mixed clastic rocks and their metamorphosed equivalents. They may also occur as carbonate replacement ores within a clastic-rock-dominated sedimentary sequence.

The vast majority of clastic-dominated deposits globally occur in Proterozoic basins that formed between 2.02 billion years ago—the age of the earliest known deposit of these ores—and about 1.85 to 1.58 billion years ago, which reflects a major period of clastic-dominated lead-zinc deposition in Australia and India. The appearance of clastic-dominated deposits in the Precambrian period corresponds to a time of formation of large and long-lived basins on stable cratons that followed the Great Oxidation Event at about 2.4 to 1.8 billion years ago. The formation of clastic-dominated deposits is related to enhanced oxidation of sulfides in the crust (which released sulfate to the hydrosphere and lead and zinc to sediments); the development of major redox and compositional gradients in the oceans; the first formation of significant sulfate-bearing evaporates, red beds, and oxidized aquifers; and the evolution of sulfate-reducing bacteria (Leach, Bradley, and others, 2010, p. 593). A number of clastic-dominated lead-zinc deposits also formed during the Carboniferous Period along passive margins in sedimentary-evaporite belts of Pangea and were deposited after the second oxidation event.

Mineralogical and geochemical evidence suggests that clastic-dominated ore fluids were principally hot metalliferous basinal brines (for example, Badham, 1981; Lydon, 1983; Cooke and others, 2000). For example, the brines that deposited sphalerite at the Red Dog deposit in Alaska had temperatures in the range of 100 to 200 °C and salinities from 14 to 19 weight percent NaCl equivalent (Leach, Marsh, and others, 2004). The dominant sulfide minerals present are sphalerite (which is generally the most common sulfide mineral) and lesser amounts of galena and the iron sulfides, marcasite, pyrite, or pyrrhotite; chalcopyrite and sulfosalt minerals may be present in minor amounts (Large, 1981, 1983; Lydon, 1983; Large and others, 2005). The sulfide minerals form lens-like bodies that are interbedded with fine-grained dark clastic and chemical sedimentary rocks. Carbonate minerals (ankerite, calcite, dolomite, and siderite), barite and quartz, siliceous shale, and low-grade silica-replaced rocks are common and can be gradational into massive ore. Ore from these deposits (table H4) generally contains less than 100 ppm gallium, with a typical range of 5 to 50 ppm gallium (table H2). For example, the Red Dog deposit (fig. H4) is hosted by organic-rich mudstone and shale of the Mississippian Kuna Formation (Kelley and others, 2004), and zinc concentrate from the deposit has 26 ppm gallium (Alaska Department of Environmental Conservation, 2005). Other elements in association with clastic-dominated lead-zinc deposits include Ag, Al, As, Au, B, Ba, Cd, Co, Cu, Fe, Ge, Hg, Mn, Mo, Ni, and Sb (Briskey, 1986; Kelley and others, 1995).

Mississippi Valley Lead-Zinc Type

Carbonate-hosted lead-zinc deposits are found throughout the world, and large famous examples occur in central North America; hence, they are generally referred to as Mississippi Valley-type deposits. The most important characteristics of Mississippi Valley-type deposits (Sangster, 1990; Leach and Sangster, 1993; Leach, Sangster, and others, 2005) are that they occur globally in dolostone and limestone that formed in platform carbonate sequences. They are commonly related to extensional domains inboard of contractional tectonic belts or continental extensional basins transitional to passive margin basins (figs. H5*C* and H5*E*). The ores are usually located at flanks of basins, orogenic forelands, or foreland thrust belts inboard of the clastic-rock-dominated passive margin sequences. Numerous lines of evidence have established that the metals were carried in fluids derived mainly from evaporated seawater and driven within the carbonate sequences by large-scale tectonic events.

More than 80 percent of Mississippi Valley-type deposits are hosted by rocks formed during the Phanerozoic Eon; less than 20 percent occur in Precambrian rocks (Sangster, 1990; Leach, Bradley, and others, 2001; Leach, Sangster, and others, 2005; Kesler and Reich, 2006). Increased oxygenation of the oceans following the second oxidation event of the atmosphere in the late Neoproterozoic Era led to an abundance of evaporites, oxidized brines, and a dramatic increase in the volume of coarse-grained and permeable carbonates in Paleozoic carbonate platforms. Most Phanerozoic-hosted Mississippi Valley-type deposits formed in the carbonate platform sequences during Devonian to Permian time as a

result of tectonic events generated by the assimilation of Pangea. A lesser number formed during Cretaceous to Tertiary time when microplate assimilation affected the western margin of North America and Africa-Eurasia.

These ores consist mainly of galena, sphalerite, and generally lesser amounts of iron sulfides. Copper and silver are important constituents in some of these deposits (for example, deposits of the Irish subtype and some deposits of the Viburnum Trend). Gangue minerals are dominantly carbonates (ankerite, calcite, dolomite, and siderite), with typically minor amounts of barite. Silicification of the host rocks (or quartz gangue) is generally minor, but may be abundant in a few deposits. Minor minerals associated with Mississippi Valley-type mineralization differ widely between individual districts, and minor and trace metals also vary (Lavery and others, 1994). Minor elements and element associations can include Ag, As, Au, Ba, Bi, Cd, Co, Cu, Ga, Ge, In, Fe, Hg, Mn, Mo, Ni, Sb, Sn, and Tl (Hall and Heyl, 1968; Hagni, 1983; Viets and others, 1992; Leach, Taylor, and others, 2010).

In Mississippi Valley-type deposits, gallium is primarily in sphalerite, which typically can contain from 0.02 to more than 500 ppm gallium (table H4). The overall content of gallium in studied deposits averages about 58 ppm; however, averages for individual deposits can vary widely, from 6 to 130 ppm gallium.

Kipushi Polymetallic Type

Kipushi-type deposits are relatively rare, epigenetic, discordant deposits of Cu–Zn–Pb–Ag–As–Sb–Ge–Ga-bearing ores that occur in carbonate platform rock sequences and are typically associated with karst, solution collapse breccias, and related features, such as salt diapirs (fig. H5*F*; Hitzman and others, 2005). The most important characteristics of these deposits are their geologic setting and distinctive polymetallic mineralogy. Considerable controversy remains concerning whether these deposits have an igneous affinity; however, most are classified as sediment-hosted deposits. Deposits of the Kipushi type (fig. H4) include world-class polymetallic orebodies at Tsumeb and Khusib Springs in Namibia (Söhnge, 1964), and at Kipushi (in the Democratic Republic of the Congo) in the Zaire-Zambia copper belt (Intiomale and Oosterbosch, 1974). Domestic deposits of this type include orebodies at the Ruby Creek Mine in Alaska (Hitzman, 1986; Bernstein and Cox, 1986; Selby and others, 2009) and at the Apex Mine in Utah (Bernstein, 1986). Other large deposits included in this group in the past are, in Australia, the Mount Isa Mine in the State of Queensland, and the Cooley and Ridge deposits of the McArthur River Mine in the Northern Territory (Bernstein and Cox, 1986; Hitzman, 1986; Selby and others, 2009); more recent studies, however, suggest that these deposits are better classified as clastic-dominated-type deposits because they are mainly lead-zinc orebodies in dolomitic siltstones, mudstones, and sandstones formed in a continental sag basin (Cooke and others, 2000; Leach, Marsh, and others, 2005; Leach, Bradley, and others, 2010; Taylor and others, 2009).

Features of Kipushi-type deposits that are similar to aspects of clastic-dominated-type and Mississippi Valley-type deposits include the general platform carbonate setting, a lack of spatially associated igneous intrusions, regional-scale ore fluid migration (as evidenced by the widespread occurrence of mineralization over thousands of square kilometers in the largest deposits), and ore localization in solution collapse breccias. The orebody at Kipushi-type deposits forms a highly irregular subvertical pipe at the faulted boundary of dolomitic shale and marine dolomite, commonly within breccia zones, and prospecting for copper-rich ores is focused on paleokarst structures that are possibly related to salt diapirs (Intiomale and Oosterbosch, 1974). The Khusib Springs deposit, which is a lens-shaped sulfide orebody up to 10 meters in thickness and elongated parallel to the bedding, replaces locally brecciated limestone of the lower Tsumeb subgroup. The origin of the breccia pipes is probably related to the erosion and karstification of the Hüttenberg Formation (Hughes and others, 1984; Hughes, 1987); however, there is some evidence that hydrothermal brecciation and silicification occurred during mineralization (Chetty and Frimmel, 2000; Kamona and Günzel, 2007). Fluid inclusion studies have also established that mineralizing fluids for Kipushi-type deposits are comparable to or higher than those of typical Mississippi Valley-type deposits and clastic-dominated lead-zinc deposits (see above). Ore-stage minerals contain highly saline fluids (17 to 43 weight percent NaCl equivalent) in inclusions with homogenization temperatures that vary from about 100 to 380 °C; the fluids were generated in postorogenic, extensional settings (Misiewicz, 1988; Chetty and Frimmel, 2000; Selby and others, 2009; Haest and others, 2009; van Wilderode and others, 2012).

Kipushi-type deposits are distinguished from Mississippi Valley-type deposits by having significantly higher trace element concentrations and more diverse mineralogy (Frimmel and others, 1996). Primary minerals include enargite, galena, and pyrite, and a zinc-rich tennantite; locally abundant zones of bornite, chalcocite-digenite, and chalcopyrite; galena, pyrite (cobaltiferous), pyrrhotite, and iron-poor sphalerite. Late-stage phases include carrollite and copper-thiogermanate minerals, pearceite-polybasite, native silver, tetrahedrite, and silver-tennantite. Additional minerals identified in some deposits include covellite, a tungsten-bearing germanite, germanium-bearing stannoidite, and stromeyerite. Gangue minerals include barite and barium-silicate minerals, calcite, chlorite, dolomite, fluorite, sparse quartz, and siderite. Ore minerals in Kipushi-type deposits can have gallium contents that range from hundreds of parts per million gallium to about 60 weight percent gallium (tables H2 and H3). Compared with other sediment-hosted ore systems, Kipushi-type deposits are characterized by marked enrichments in germanium and rhenium (Schneider and others, 2007). Many weathered deposits of this type contain gallium-bearing secondary minerals formed largely through supergene processes (table H3). For example, at the Apex Mine in Utah, the primary ore is inferred to be similar

to bornite-chalcopyrite-tennantite-galena-sphalerite ore of a Kipushi type, although the Apex orebodies are almost completely oxidized to germanium-bearing hydrogoethite and gallium-bearing (up to about 1 percent gallium) jarosite.

Resources and Production

Identified Resources

The U.S. Geological Survey (USGS) estimates that world resources of gallium in bauxite exceed 1 billion kilograms and that a considerable quantity of gallium could be present in world zinc resources (Bray, 2013). Using USGS information coupled with data on global bauxite provinces (Bogatyrev and Zhukov, 2009), comparable estimates of geologically available gallium in bauxite reserves and resources (of nearly 1.4 million metric tons and 4 million metric tons, respectively) have been suggested (Dittrich and others, 2011). Analogous estimates of world resources of gallium in zinc resources have not been made owing to insufficient data. The United States is expected to meet its current and expected future needs for gallium through imports of primary gallium from these resources, from imports of recycled and refined gallium, and from domestic production of recycled and refined gallium.

Identified bauxite resources of the world are about 55 to 75 billion metric tons and occur in Africa (32 percent), Oceania (23 percent), South America and the Caribbean (21 percent), Asia (18 percent), and elsewhere (6 percent) (Bray, 2012). Lateritic bauxite deposits make up approximately 90 percent of global bauxite resources, and aluminum production is mainly from these deposits (Freyssinet and others, 2005). Karst bauxite deposits are more scattered in distribution and are mined mainly in eastern Europe and the Caribbean islands (Bárdossy, 1982). Domestic bauxite deposits consist mainly of subeconomic resources that are not generally suitable for alumina production owing to their high silica content; thus, recovery of gallium from these deposits is unlikely. Although domestic resources of bauxite are inadequate to meet either short- or long-term U.S. demand, the United States has essentially inexhaustible subeconomic resources of aluminum in materials other than bauxite. These are primarily clay deposits, which also contain gallium in amounts comparable to those of bauxite (30 to 50 ppm gallium) (table H2). Identified zinc resources of the world are about 1.9 billion metric tons (Tolcin, 2013). Mississippi Valley-type deposits, which are widespread in North America, account for about 38 percent of the global resources of lead and zinc in sediment-hosted ore deposits; significant zinc resources are also contained in clastic-dominated deposits of Alaska (fig. H4; Leach, Marsh, and others, 2005).

The estimates given here apply to total gallium content; only a small percentage of gallium metal in bauxite and zinc ores is recoverable using current methods because processing techniques to separate aluminum, zinc, and other byproduct metals (for example, germanium and indium) compete for gallium in source materials. Factors controlling gallium recovery are typically proprietary, and scant literature is available on the general operating practices of companies involved in gallium production. The potential remains for additional gallium production given more efficient and improved extraction technologies and market-driven economic incentives.

Undiscovered Resources

The USGS has conducted no quantitative mineral resource assessments focused on undiscovered domestic or global resources of bauxite since the work of Patterson and others (1986). Because the major bauxite provinces of the world are well established and have been intensely explored, most of the significant bauxite deposits globally are thought to be known (Freyssinet and others, 2005). The major bauxite provinces (fig. H4) occur in the following five major regions: (a) the South American region—the Guiana shield (French Guiana, Guyana, Suriname) and the central Brazilian shield; (b) the West African region—Burkina Faso, Ghana, Guinea, Ivory Coast, Mali, and Sierra Leone; (c) the Indian region—the western and eastern coasts; (d) Southeast Asia—Cambodia, Laos, and Vietnam; and (e) the Australian region. Other bauxite provinces occur in the southern United States (Arkansas region), the Caribbean, the southern Ural Mountains (Russia and Kazakhstan), and China.

The most recent USGS National Mineral Resource Assessment identified areas of the United States that have significant potential for undiscovered resources of zinc (Schruben, 2002). The estimate of the amount of zinc in undiscovered U.S. deposits ranged from a 90-percent probability of at least 130 million metric tons to a 10-percent probability of at least 290 million metric tons. The mean estimate of zinc in undiscovered deposits was 210 million metric tons. Nearly 40 percent of the zinc was thought to be contained in undiscovered Mississippi Valley-type deposits. Other major deposit types were sedimentary exhalative (31 percent), volcanogenic massive sulfide (15 percent), and polymetallic replacement (8 percent) deposit types. At that time, the total identified zinc resources in the United States were estimated to be 99 million metric tons. No comparable estimates of undiscovered global resources of zinc have been made.

Production

In 2012, world primary gallium production was estimated to be 273 metric tons (fig. H4*A*). China, Germany, Kazakhstan, and Ukraine were the leading producers; countries with lesser output were Hungary, Japan, the Republic of Korea, and Russia. Refined gallium production was estimated to be about 354 metric tons; this estimate includes primary gallium production and some scrap refining. China, Japan, the United Kingdom, and the United States were the principal producers of refined gallium. Gallium was recycled from new scrap in Canada, Germany, Japan, the United Kingdom, and

the United States. World primary gallium production capacity in 2012 was estimated to be 474 metric tons; refinery capacity, 270 metric tons; and recycling capacity, 198 metric tons (Jaskula, 2013a). Imports of gallium into Japan and the United States (the two leading consuming countries) were used as the basis for estimating world gallium production. In addition, Metal Bulletin (2013) provided an updated Chinese gallium production estimate, expanding the estimate of China's production considerably owing to the substantial capacity increases of China's gallium operations (fig. H4*B*).

No domestic production of primary gallium was reported in 2012. Molycorp Inc. recovered gallium from scrap materials, predominantly those generated during the production of GaAs. Molycorp's facility in Blanding, Utah, has the capability to produce about 50 metric tons per year of high-purity gallium. The company recovered gallium from its customers' scrap on a fee basis and purchased scrap and low-purity gallium for processing into high-purity material.

Exploration for New Deposits

Most domestic exploration for gallium is done as a second-order effort related to new discoveries of zinc resources because U.S. bauxite resources are currently subeconomic. Exploration is active in the United States and globally for all types of large-tonnage zinc deposits, which constitute a major source for gallium (Emsbo, 2009; Taylor and others, 2009; Leach, Bradley, and others, 2010). There is some evidence that partitioning of gallium may be influenced by the amount of sphalerite in bulk ore, leading to a dilution effect, such that the largest zinc deposits of a given type may be expected to have relatively lower gallium contents (Cook and others, 2009). This, however, may have little effect on resource estimation because economic factors that support gallium extraction are tilted in favor of large tonnage values for the principal commodity over small changes in grade for a byproduct element. The most gallium-enriched sediment-hosted ores are the Kipushi-type deposits, which are mined for copper, lead, silver, and zinc and byproduct antimony, arsenic, germanium, and gallium; some deposits of this group may contain gallium (and germanium) in amounts that justify extraction as a primary product. Active exploration efforts are underway in the major Kipushi-type provinces of the Central African copperbelt—Kipushi and Tsumeb. Important domestic examples of Kipushi-type deposits include the Ruby Creek deposit in Alaska and the Apex deposit in Utah. Additional domestic exploration efforts are focused on gallium resources associated with epithermal mineralized and hydrothermally altered volcanic rock suites.

Ruby Creek deposit, Alaska.—This deposit is located along the northern flank of the Cosmos Hills near the boundary between a carbonate platform and a shale basin within the Ambler district. The 1-kilometer-diameter body of hydrothermal dolostone is one of several similarly mineralized occurrences in the Cosmos Hills. The Ruby Creek deposit contains more than 90 million metric tons of 1.2 percent copper, plus elevated contents of silver, cobalt, germanium, gallium, and zinc (Hitzman, 1986). The metacarbonate sequence consists primarily of thin-bedded to massive metadolostone and marble that is locally graphitic or phyllitic and contains thin micaceous layers interpreted as airfall tuffs (Hitzman, 1986; Hitzman and others, 1986). The presence of coeval volcanogenic massive sulfide deposits just north of the Ruby Creek deposit is possible evidence for regionally extensive hydrothermal activity, perhaps related to igneous activity associated with continental extension (Hitzman and others, 1986; Selby and others, 2009).

Apex deposit, southwestern Utah.—This deposit has served as the only primary source in the world for the production of gallium and germanium. The Apex Mine operated intermittently from 1884 to 1962, and more than 7,000 metric tons of copper, 5,600 kilograms of silver, and small amounts of gold and lead were produced. The mine was reopened in 1985 with plans to produce gallium and germanium (Washington County Historical Society, 2013). At that time, the mine was estimated to contain 220,000 metric tons of ore grading 0.064 percent germanium, 0.032 percent gallium, 1.63 percent copper, 0.77 percent lead, 1.58 percent zinc, 0.50 percent arsenic, 16.73 percent iron, and 38 grams per metric ton silver (Bernstein, 1986). Surface dumps from the old mine contained an additional 45,000 metric tons of material grading 0.037 percent germanium, 0.019 percent gallium, and 1.55 percent copper. Similar deposits may occur in association with copper in fault-hosted breccias in Pennsylvanian limestone near Hansonburg, New Mexico (Eveleth and Lueth, 2009).

Cordero Gallium Project, Humboldt County, Nevada.—This project is reportedly North America's largest known primary gallium occurrence (Rêserva International LLC, 2008). Anomalous gallium mineralization occurs over a wide area in and around the historic Cordero and McDermitt mercury mines. There are indications that a number of high-grade "feeder zones" occur through the deposit, which also hosts significant occurrences of rare-earth elements. The resources for the project above a cutoff grade of 30 ppm gallium are estimated to exceed 13 million metric tons (Rêserva International LLC, 2008).

Environmental Considerations

Sources and Fate in the Environment

In weathering environments, gallium is generally immobile and is only slightly less reactive than aluminum (Shiller and Frilot, 1996). The tendency for gallium to be dissolved and transported depends upon its chemical form, which in turn depends largely upon the pH and temperature of weathering solutions. Gallium associated with bauxite at a pH near 4 and a weathering solution temperature of 25 ºC would be expected to remain as a solid (for example, $Ga(OH)_3$

or GaO(OH)), but can theoretically dissolve to form aqueous hydroxide complexes ($Ga(OH)_3$ or $Ga(OH)_4$ at pH values > 4 and Ga(OH) and $Ga(OH)_2$ at pH values < 4; Bénézeth and others, 1997; Diakonov and others, 1997). Gallium is expected to be transported in soils, streams, and rivers in the solid phase as small particulates because of the low solubility of gallium minerals in natural waters.

Gallium associated with sulfide minerals is more mobile based on the instability of sulfides at Earth's surface. Dissolution of sulfide minerals releases metals and sulfuric acid, and the acidic pH values allow higher concentrations of metals to be dissolved in solution—potentially causing the environmental problem known as acid mine drainage (AMD). Under acidic conditions, gallium would most likely form dissolved complexes with sulfate and (or) chloride (for example, $GaSO_4^+$ or $GaCl^-$) (Wood and Samson, 2006). Metals dissolved in AMD can be naturally attenuated through precipitation, sorption to oxyhydroxide minerals, or dilution by mixing with water at circumneutral pH; otherwise, metals are transported downstream.

Examples of natural concentrations of gallium in soil, water, and air are given in table H2. Gallium contents in soils range from 3 to 70 milligrams per kilogram (mg/kg) (or 3 to 70 ppm) (Kabata-Pendias and Pendias, 2001), and concentrations as high as 220 mg/kg have been observed in agricultural soil (Połedniok and others, 2012). Gallium generally behaves like aluminum in the environment, but, under certain pH and redox conditions, the two elements may be separated. As a result, values of the ratio of gallium to aluminum (Ga:Al ratio) can aid in detecting gallium enrichment in various materials. Shiller and Frilot (1996) showed that the Ga:Al ratio of parent rocks (and residual soils) and streambed solids were similar, whereas the Ga:Al ratio in nearby streams was higher than those in parent rocks. The concentration of gallium in these streams ranged from 0.0001 to 0.006 micrograms per liter (µg/L) (or 0.0001 to 0.006 parts per billion). These concentrations are generally lower than the 0.001 to 0.12 µg/L range of dissolved gallium found in large rivers around the world and are comparable to gallium concentrations measured in the Atlantic Ocean (Shiller, 1998). Compared with dissolved species, gallium is highly concentrated in small particulates in river water, with a global average of 18.1 mg/kg in suspended sediment (Viers and others, 2009). Gallium occurs naturally in the atmosphere as part of mineral dust particles and has been measured to be less than 0.14 nanograms per cubic meter (ng/m^3) at the South Pole (Kabata-Pendias and Pendias, 2001).

Mining and ore processing can hasten the weathering process and can lead to above-background concentrations of gallium in soil and water (table H2). For example, gallium concentrations ranging from 93 to 270 mg/kg have been observed in soils near bauxite and lead-zinc mine sites in Poland (Połedniok and others, 2012). In addition, anthropogenic release of gallium to the atmosphere occurs during coal combustion, ore processing, and semiconductor manufacturing, leading to concentrations as high as 1 to 12 ng/m^3 near industrial areas (Chen, 2007; Kabata-Pendias and Mukherjee, 2007). Likewise, dissolved and colloidal concentrations of gallium in groundwater near semiconductor manufacturing areas in China have been measured to be greater than 10 µg/L (Chen, 2006). The recycled content, or proportion of scrap, used in gallium production is between 10 and 25 percent, but the fraction of gallium in discarded products that get recycled is less than 1 percent (Graedel and others, 2011). One of the main challenges of gallium recycling is that it is commonly comingled with other "specialty metals" in high performance alloys, making recovery technologically and economically unfeasible (Reck and Graedel, 2012). Given the importance of gallium in thin-film photovoltaic cells and integrated circuits, however, gallium recycling is likely to increase in the future (Graedel, 2011).

Mine Waste Characteristics

Mine waste is generally considered to be the material that originates and accumulates at a mine site that has no current economic value (Lottermoser, 2010), and it includes both solid and liquid waste. Gallium associated with bauxite is usually mined by open pit or underground methods and then refined through the Bayer process, which can lead to large volumes of processing waste. Based on its appearance, bauxite (or alumina) processing waste is commonly referred to as red mud. Red mud depositories are connected with alumina processing plants and are not necessarily located at the mine site. For example, four active plants in the United States predominantly process alumina ore from overseas (Bray, 2012). On October 4, 2010, a breached red mud depository released between 600,000 to 700,000 cubic meters of material from the Ajka Timfoldgyar Zrt alumina plant in Hungary (Reeves and others, 2011). This spill was unprecedented both in scale (the spill covered an estimated 800 hectares of land [Ruyters and others, 2011]) and in its delivery of trace elements across such a vast area (Mayes and others, 2011).

Bauxite ore results from extreme chemical weathering, and many elements that were originally present in the parent rock have been leached away. The exceptions are minor elements that can sorb to or coprecipitate with aluminum and iron (oxyhydr)oxide minerals that make up the ore and waste. For example, in addition to Al and Fe, bauxite processing waste has been shown to contain elevated concentrations of As, Cr, Ga, Mo, Ni, and V (Mayes and others, 2011). Bauxite mine and processing waste generally lacks acid-generating minerals, so these elements are expected to remain immobile under oxidizing and near-neutral ($5 < pH < 8$) weathering conditions as long as abundant iron-rich particles are present (Smith and Huyck, 1999).

Waste products that result from mining sediment-hosted deposits usually consist of waste rock, tailings piles, and possibly pit lakes. For example, the cumulative volume of tailings generated at the Red Dog Mine, which is a clastic-dominated lead-zinc deposit, totaled 27.4 million metric tons in 2006, and it is projected to total 88 million metric tons

by 2031 (SRK Consulting [Canada] Inc., 2007). The largest U.S. Environmental Protection Agency Superfund site occurs in the Tri-State zinc mining district and contains an estimated 91 million metric tons of waste rock (U.S. Environmental Protection Agency, 2006). The district contains a large number of Mississippi Valley-type lead-zinc deposits and covers approximately 1,800 square kilometers of Kansas, Oklahoma, and Missouri (Leach, Taylor, and others, 2010). The mineralogy of the mine waste associated with these deposits reflects the mineralogy of the unmined deposit, except that the proportion of lead-zinc-copper sulfides, such as chalcopyrite, galena, and sphalerite, is reduced relative to the gangue minerals (barite, calcite, dolomite, pyrite, and quartz) (Kelley and others, 1995; Leach, Viets, and others, 1995). Because of their association with sulfides and secondary minerals, such elements as Ag, Al, As, Au, B, Ba, Cd, Co, Fe, Ga, Ge, Hg, Mn, Mo, Ni, and Sb can also be found in clastic-dominated deposits (Briskey, 1986; Kelley and others, 1995). Likewise, Mississippi Valley-type deposits can contain minor to trace amounts of Ag, As, Au, Ba, Bi, Cd, Co, Cu, F, Fe, Ga, Ge, In, Mo, Ni, Pb, Sb, Sn, and Tl (Leach, Viets, and others, 1995; Foley, 2002a). Under oxidizing and acidic ($pH < 3$) weathering conditions, which would be expected in clastic-dominated mine waste having little to no acid-neutralizing capacity and significant pyrite content, many of these elements are mobile (Smith and Huyck, 1999). The acid-neutralizing capacity of carbonate-hosted mine waste is greater, however, and the oxidizing and circumneutral ($5 < pH < 8$) conditions that prevail during weathering would cause most of the elements listed above to be less mobile or immobile (Smith and Huyck, 1999). An important exception is zinc, which can make up a large percentage of the total dissolved metals draining from Mississippi Valley-type deposits (Plumlee and others, 1999). A review of the environmental geochemistry of platform carbonate-hosted sulfide deposits identifies surface disposal of tailings as a potential environmental concern, especially if As, Cd, Tl, and Zn are present, because airborne dust may contain metal particulates (Foley, 2002a). A study of the Austinville lead-zinc mine in Wythe County, Virginia (Foley, 2002b), shows that residual soils near a Mississippi Valley-type deposit can be acidic enough to influence the mobility of metals in surface environments and that this is especially true for Mississippi Valley-type deposits that have high jasperoid and pyrite content.

Human Health Concerns

Study of the health effects of gallium on humans largely focuses on exposure to synthetic gallium arsenide (GaAs) by workers in the semiconductor industry, where small GaAs particles can be inhaled or ingested (Flora, 2000). The toxicity of GaAs may result from the arsenic (because arsenic trioxide may be released from GaAs after absorption); gallium toxicity, however, though not well studied, has not been ruled out (Chitambar, 2010). Humans can tolerate intravenous infusions of gallium nitrate during medical treatments for diseases such as cancer (Chitambar, 2010), but the long-term effects of human exposure to gallium in drinking water and soil resources remain unknown. Gallium does not appear in the U.S. Clean Water Act, and the Occupational Safety and Health Administration (OSHA) does not consider gallium metal to be hazardous, although some State governments include gallium in their right-to-know lists (Ziegler and others, 2004).

Given their similar chemical characteristics, the health effects of gallium may be similar to those of aluminum. The Agency for Toxic Substances and Disease Registry (ATSDR) provides a useful summary of the human toxicology of aluminum (Agency for Toxic Substances and Disease Registry, 2008). Exposure to aluminum by the general public is most likely to occur through consumption of food, water, and aluminum-bearing medicines (such as antacids or antidiarrheal agents). Occupational exposure to aluminum is most likely to occur during ore processing and product fabrication. Most ingested or inhaled aluminum is not absorbed by the body, although absorption can vary depending upon the chemical form and particle size. Overexposure to aluminum can affect the nervous system, causing impaired performance in motor, sensory, and cognitive function. In addition, aluminum workers may suffer respiratory effects, such as impaired lung function and fibrosis. The United States national secondary drinking water regulation for aluminum, which is a nonenforceable guideline, ranges from 50 to 200 µg/L (U.S. Environmental Protection Agency, 2013b). Most surface waters contain aluminum concentrations below 100 µg/L (Agency for Toxic Substances and Disease Registry, 2008).

Mining of deposits where gallium is a byproduct can potentially mobilize elements that are known human toxins; these elements have the potential to affect human health when present above threshold concentrations in air, drinking water, and soils. These concentrations can be exceeded near mine sites. The best known examples are the neurological effects of lead on children (Holecy and Mousavi, 2012) and the carcinogenic effects of arsenic in drinking water (Gupta and others, 2012). The current U.S. National Ambient Air Quality Standard for lead is 0.15 micrograms per cubic meter (U.S. Environmental Protection Agency, 2013a), and current U.S. primary and secondary drinking water standards for lead, zinc, and copper are 0, 5, and 1 milligrams per liter (mg/L), respectively (U.S. Environmental Protection Agency, 2013b). Canadian agricultural soil quality guidelines for lead, zinc, and copper are 70, 200, and 63 mg/kg, respectively (Canadian Council of Ministers of the Environment, 2007).

Ecological Health Concerns

Relatively few studies focus on the ecological effects of gallium mobility in the environment. Fish tend to be sensitive to low concentrations of dissolved metals, and they are therefore useful indicators of contamination in aquatic systems. One of several useful endpoints used in toxicity tests is the lethal concentration that leads to 50 percent mortality (LC_{50}) after exposure to a substance for a certain amount of time.

A study on the acute toxicity of dissolved gallium to carp (*Cyprinus carpio Linnaeus*) revealed a mean LC_{50} value of 95.6±14.3 mg/L after 96 hours of exposure (Betoulle and others, 2002). Chronic toxicity tests with dissolved gallium and developing rainbow trout (*Oncorhynchus mykiss)* revealed a mean LC_{50} value of 3.5 mg/L after 28 days of exposure (Birge and others, 1980). In acute toxicity tests with saltwater organisms, LC_{50} values ranged from 12 to 55 mg/L of gallium after 24, 48, or 96 hours of exposure (Onikura and others, 2005). Gallium is typically not included in the suite of elemental concentrations reported in studies of mine waste water chemistry, so these LC_{50} values cannot be compared with likely gallium concentrations in mining environments.

The ecological effects of gallium may be similar to those of aluminum given their similar behavior in the environment. When brown trout (*Salmo trutta Linnaeus*) were exposed to stream water samples of various pH levels and aluminum concentrations, the healthiest populations were observed in waters with pH above 5.0 and aluminum concentrations below 20 µg/L; significantly higher aluminum concentrations in gills were observed in moribund fish, suggesting that complications with respiration contributed to their decline (Andrén and Rydin, 2012). In toxicity tests with tropical freshwater algal and zooplankton species, LC_{50} values for aluminum increased with increasing dissolved organic carbon concentrations (Trenfield and others, 2012), suggesting that the affinity of aluminum for complexing with organic carbon renders it less toxic. The National Ambient Water Quality Criteria recommended for the protection of aquatic life and adopted by some regions in the United States are 750 micrograms of aluminum per liter (µg Al/L) of water (acute) and 87 µg Al/L of water (chronic) (Suter and Tsao, 1996). Because aluminum is more mobile under acidic conditions, plants growing in acidic soils may suffer from aluminum toxicity, which is known to inhibit root growth and crop yields (Kabata-Pendias and Mukherjee, 2007). As a result, some regions of the United States have adopted a soil screening benchmark of 50 ppm of soil for terrestrial plants, as recommended by Oak Ridge National Laboratory (Efroymson and others, 1997).

The ecological effects of other elements that gallium is associated with are relatively well documented. For example, in toxicity tests with aquatic invertebrates incubated with mine tailings from Mississippi Valley-type deposits, Besser and Rabeni (1987) showed that increased concentrations of dissolved cadmium, lead, and zinc correlated with decreased survival and growth (Besser and Rabeni, 1987). Likewise, various fish species experienced rapid mortality when exposed to increasing dissolved zinc concentrations, but this effect decreased with increasing calcium, magnesium, and sodium concentrations (De Schamphelaere and Janssen, 2004). High metal concentrations in soils can also cause phytotoxicity. Zinc is a micronutrient for many plant species, but when highly concentrated in soils, it can inhibit a plant's metabolic functions and cause deficiencies in other essential nutrients, such as copper, iron, manganese, and phosphorus (Nagajyoti and others, 2010, and references therein).

Carbon Footprint

Gallium has potential application in the effort to reduce the carbon footprint from energy production because of its use in efficient thin-film photovoltaic cells (solar panels) (Miles and others, 2007). The copper-indium-gallium-(di)selenide (CIGS) alloy, among others, is an attractive thin-film product because of its high efficiency and relatively low material and manufacturing costs (Kaneshiro and others, 2010). In a comparative study of lifecycle greenhouse gas emissions for various technologies, Kim and others (2012) found that estimates for the carbon footprint of CIGS technologies under test conditions are about 26 grams of CO_2 equivalent per kilowatthour (g CO_2-equiv/kWh), which compares well with older technologies that have greenhouse gas emissions in the range of 39 to 110 g CO_2-equiv/kWh (Fthenakis and others, 2008). The CIGS photovoltaic cells are in the initial stages of commercialization, but they are expected eventually to compete with other forms of energy production as economies of scale permit future cost reductions (Miles and others, 2007; Rockett, 2010). With the rapid evolution of the thin-film photovoltaic cell industry, the recyclability of generated products and the potential for leaching of toxic elements from improperly disposed products would need to be addressed.

Mine Closure

Most recent and new mining operations include closure plans that address issues related to the mine footprint, which includes waste left onsite and locally affected soil and water, as well as ecological effects, such as habitat destruction and loss of biodiversity. Bauxite mines can be particularly prone to soil and habitat loss given that many are located in tropical, biodiverse locations. A study of a 10-year-old reforested area at a closed bauxite mine in Brazil showed that, although the reforestation program created adequate recovery conditions, recovery of native flora was influenced by the uneven return of important seed-dispersing animals (Parrotta and others, 1997). At one of the largest bauxite mine operations in the State of Western Australia, Australia, the Alcoa World Alumina Australia company clears the Jarrah (*Eucalyptus marginata*) forest before developing an open pit mine; after extracting bauxite, the company returns the topsoil and spreads Jarrah seeds at a rate of approximately 550 hectares per year (Gardner and Bell, 2007).

With respect to mining in zinc deposits, mine closure issues often relate to the stability of large waste piles and tailings dams, and the potential for acid mine drainage from the site. Mine waste pile stability is commonly addressed through grading and covering dewatered piles. Acid mine drainage can be addressed with active water treatment facilities, passive limestone-lined channels, or constructed wetlands (Plumlee and Logsdon, 1999). The end result of both active and passive approaches is precipitation of dissolved metals. Precipitated metals in reconstructed wetland systems tend to be more stable under the prevailing anoxic conditions,

whereas the metal-rich precipitates that result from active treatment facilities form a sludge that can be similar to the metal-rich bauxite processing residues. At large mines, mine waste is typically consolidated into pits and submerged under water, forming a tailings pond. Acid-generating minerals are less reactive under water, but seepage is typically monitored and, if necessary, treated. At such sites as the Red Dog Mine in Alaska, seepage from the tailings ponds may need to be treated in perpetuity (U.S. Environmental Protection Agency, 2010). Failure of tailings pond impoundments can cause catastrophic flooding (McDermott and Sibley, 2000). Thus, plans for securing waste piles and prevention and treatment of acid mine drainage are important aspects of long-term active and proposed metal mining projects.

Problems and Future Research

Future research efforts related to gallium resources are likely to be directed at understanding the factors that may affect future supplies. Such research could include developing improved assessment models, conducting experimental studies, and seeking new and more efficient extraction and recycling technologies.

Assessment models.—Improved models could help in locating new and unconventional resources. Efforts focused on incorporating additional geochemical and mineralogical data into existing mineral deposit and grade tonnage models (for zinc and bauxite deposits) can contribute to the development of quantitative grade-tonnage models and new approaches to evaluating the geologic availability of gallium as a byproduct. New models to estimate the occurrence of gallium in polymetallic resources of the Kipushi type could also contribute to more accurate quantitative assessments of the geologic availability of gallium. Also, models can assist in the evaluation of resources of gallium currently locked up in unprocessed mine waste, such as the extensive waste piles left over from the mining of Mississippi Valley-type deposits in the mid-continent region of the United States.

Experimental studies.—Studies of gallium at conditions applicable to biochemical processes occurring in surface environments would provide for a better understanding of the natural gallium lifecycle and the potential issues related to gallium waste disposal.

New technologies.—Devising new and more efficient extraction technologies for both raw ore and recycled products would help prevent or alleviate future bottlenecks in the supply chain that may result from increased demand.

Recycling.—Because so little gallium in used products gets recycled, greater gallium recycling efficiency in the future can reduce reliance on mining of primary gallium resources. Future research could be focused on improving gallium recycling from current products, as well as future product design that allows greater gallium recycling efficiency.

References Cited

Note: All Web links listed were active as of the access date but may no longer be available.

Agency for Toxic Substances and Disease Registry, 2008, Toxicological profile for aluminum: Atlanta, Ga., U.S. Department of Health and Human Services, Public Health Service, September, 310 p. plus 4 appendixes. [Also available at http://www.atsdr.cdc.gov/ToxProfiles/tp22.pdf.]

Alaska Department of Environmental Conservation, 2005, table 2–1, Composition of Red Dog lead and zinc concentrates, accessed March 6, 2013, at http://dec.alaska.gov/spar/csp/docs/reddog/03dmts_ra_tables-april2005.pdf.

Andrén, C.M., and Rydin, E., 2012, Toxicity of inorganic aluminum at spring snowmelt—In-stream bioassays with brown trout (*Salmo trutta* L.): Science of the Total Environment, v. 437, p. 422–432. [Also available at http://dx.doi.org/10.1016/j.scitotenv.2012.08.006.]

Ayuso, R.A., Foley, N.K., Seal, R.R., II, Bove, Marianna, Civitillo, Diego, Cosenza, Antonio, and Grezzi, Giuseppe, 2013, Lead isotope evidence for metal dispersal at the Callahan Cu-Zn-Pb mine—Goose Pond tidal estuary, Maine, USA: Journal of Geochemical Exploration, v. 126–127, p. 1–22 . [Also available at http://dx.doi.org/10.1016/j.gexplo.2012.12.013.]

Badham, J.P.N., 1981, Shale-hosted Pb-Zn deposits—Products of exhalation of formation waters?: Institution of Mining and Metallurgy, Transactions, Section B—Applied Earth Science, v. 90, p. B70−B76.

Bárdossy, György, 1982, Karst bauxites—Bauxite deposits on carbonate rocks: Amsterdam, Netherlands, and New York, N.Y., Elsevier Scientific Pub. Co., 441 p., 5 pls. and 4 app. in pocket.

Bárdossy, György, and Aleva, G.J.J., 1990, Lateritic bauxites: New York, N.Y., Elsevier, Developments in Economic Geology Series, v. 27, 624 p., 24 pls.

Barton, P.B., Jr., and Bethke, P.M., 1987, Chalcopyrite disease in sphalerite—Pathology and epidemiology: American Mineralogist, v. 72, nos. 5–6, p. 451–467.

Bénézeth, Pascale, Diakonov, I.I., Pokrovski, G.S., Dandurand, J.-L., Schott, Jacques, and Khodakovsky, I.L., 1997, Gallium speciation in aqueous solution. Experimental study and modelling—Part 2. Solubility of α-GaOOH in acidic solutions from 150 to 250 ºC and hydrolysis constants of gallium (III) to 300 ºC: Geochimica et Cosmochimica Acta, v. 61, no. 7, p. 1345–1357. [Also available at http://dx.doi.org/10.1016/S0016-7037(97)00012-4.]

Bernstein, L.R., 1986, Geology and mineralogy of the Apex germanium-gallium mine, Washington County, Utah: U.S. Geological Survey Bulletin 1577, 9 p. [Also available at http://pubs.er.usgs.gov/publication/b1577.]

Bernstein, L.R., and Cox, D.P., 1986, Geology and sulfide mineralogy of the Number One orebody, Ruby Creek copper deposit, Alaska: Economic Geology, v. 81, p. 1675–1689. [Also available at http://dx.doi.org/10.2113/gsecongeo.81.7.1675.]

Bernstein, L.R., and Waychunas, G.A., 1987, Germanium crystal chemistry in hematite and goethite from the Apex Mine, Utah, and some new data on germanium in aqueous solution and in stottite: Geochimica et Cosmochimica Acta, v. 51, no. 3, p. 623–630. [Also available at http://dx.doi.org/10.1016/0016-7037(87)90074-3.]

Besser, J.M., and Rabeni, C.F., 1987, Bioavailability and toxicity of metals leached from lead-mine tailings to aquatic invertebrates: Environmental Toxicology and Chemistry, v. 6, no. 11, p. 879–890. [Also available at http://dx.doi.org/10.1002/etc.5620061109.]

Betoulle, S., Etienne, J.C., and Vernet, G., 2002, Acute immunotoxicity of gallium to carp (*Cyprinus carpio* L.): Bulletin of Environmental Contamination and Toxicology, v. 68, no. 6, p. 817–823. [Also available at http://dx.doi.org/10.1007/s00128-002-0028-3.]

Birge, W.J., Black, J.A., Westerman, A.G., and Hudson, J.E., 1980, Aquatic toxicity tests on inorganic elements occurring in oil shale, *in* Gale, Charles, ed., Oil shale symposium—Sampling analysis and quality assurance, March 1979, Proceedings: Cincinnati, Ohio, U.S. Environmental Protection Agency, EPA-600/9-80-022, p. 519–534. [Also available at http://babel.hathitrust.org/cgi/pt?id=coo.31924004323303;view=1up;seq=531.]

Bogatyrev, B.A., and Zhukov, V.V., 2009, Bauxite provinces of the world: Geology of Ore Deposits, v. 51, no. 5, p. 339–355. [Also available at http://dx.doi.org/10.1134/S1075701509050018.]

Bogatyrev, B.A., Zhukov, V.V., and Tsekhovsky, Yu.G., 2009, Formation conditions and regularities of the distribution of large and superlarge bauxite deposits: Lithology and Mineral Resources, v. 44, no. 2, p. 135–151. [Also available at http://dx.doi.org/10.1134/S0024490209020035.]

Bradley, D.C., and Leach, D.L., 2003, Tectonic controls of Mississippi Valley-type lead-zinc mineralization in orogenic forelands: Mineralium Deposita, v. 38, no. 6, p. 652–667. [Also available at http://dx.doi.org/10.1007/s00126-003-0355-2.]

Bray, E.L., 2012, Bauxite and alumina [advance release], *in* Metals and minerals: U.S. Geological Survey Minerals Yearbook 2011, v. I, p. 10.1–10.13, accessed March 9, 2013, at http://minerals.usgs.gov/minerals/pubs/commodity/bauxite/myb1-2011-bauxi.pdf.

Bray, E.L., 2013, Bauxite and alumina: U.S. Geological Survey Mineral Commodity Summaries 2013, p. 26–27. [Also available at https://minerals.usgs.gov/minerals/pubs/commodity/bauxite/mcs-2013-bauxi.pdf.]

Brimhall, G.H., Chadwick, O.A., Lewis, C.J., Compston, William, Williams, I.S., Danti, K.J., Dietrich, W.E., Power, M.E., Hendricks, David, and Bratt, James, 1991, Deformational mass transport and invasive processes in soil evolution: Science, v. 255, no. 5045, p. 695–702. [Also available at http://dx.doi.org/10.1126/science.255.5045.695.]

Briskey, J.A., 1986, Descriptive model of sedimentary exhalative Zn-Pb—Model 31a, *in* Cox, D.P., and Singer, D.A., eds., Mineral deposit models: U.S. Geological Survey Bulletin 1693, p. 211–215. [Also available at http://pubs.er.usgs.gov/publication/b1693.]

Burton, J.D., and Culkin, F., 1978, Gallium, *in* Wedepohl, K.H., ed., Handbook of geochemistry, v. 2, pt. 3: Berlin, West Germany, Springer-Verlag, p. 32–D–7.

Canadian Council of Ministers of the Environment, 2007, Canadian soil quality guidelines for the protection of environmental and human health, chap. 7 *of* Canadian environmental quality guidelines: Winnipeg, Manitoba, Canada, Canadian Council of Ministers of the Environment accessed February 15, 2013, at http://www.ccme.ca/publications/ceqg_rcqe.html.

Chen, H-W., 2006, Gallium, indium, and arsenic pollution of groundwater from a semiconductor manufacturing area of Taiwan: Bulletin of Environmental Contamination and Toxicology, v. 77, no. 2, p. 289–296. [Also available at http://dx.doi.org/10.1007/s00128-006-1062-3.]

Chen, H-W., 2007, Characteristics and risk assessment of trace metals in airborne particulates from a semiconductor industrial area of northern Taiwan: Fresenius Environmental Bulletin, v. 16, no. 10, p. 1288–1294.

Chetty, D., and Frimmel, H.E., 2000, The role of evaporites in the genesis of base metal sulphide mineralisation in the Northern Platform of the Pan-African Damara belt, Namibia—Geochemical and fluid inclusion evidence from carbonate wall rock alteration: Mineralium Deposita, v. 35, no. 4, p. 364–376. [Also available at http://dx.doi.org/10.1007/s001260050247.]

Chitambar, C.R., 2010, Medical applications and toxicities of gallium compounds: International Journal of Environmental Research and Public Health, v. 7, no. 5, p. 2337–2361. [Also available at http://dx.doi.org/10.3390/ijerph7052337.]

Cook, N.J., Ciobanu , C.L., Pring, Allan, Skinner, William, Shimizu, Masaaki, Danyushevsky, Leonid, Saini-Eidukat, Bernhardt, and Melcher, Frank, 2009, Trace and minor elements in sphalerite—A LA-ICPMS study: Geochimica et Cosmochimica Acta, v. 73, no. 16, p. 4761–4791. [Also available at http://dx.doi.org/10.1016/j.gca.2009.05.045.]

Cooke, D.R., Bull, S.W., Large, R.R., and McGoldrick, P.J., 2000, The importance of oxidized brines for the formation of Australian proterozoic stratiform sediment-hosted Pb-Zn (sedex) deposits: Economic Geology, v. 95, p. 1–18. [Also available at http://dx.doi.org/10.2113/gsecongeo.95.1.1.]

Crump, M.E., 1994, A new source of gallium—Geothermal muds, *in* The Australasian Institute of Mining and Metallurgy, New Zealand Branch, 28th annual conference, Wairakei, 17–19 August 1994: Australasian Institute of Mining and Metallurgy New Zealand Branch Conference, 28th, Wairakei, New Zealand, 1994, (published in Taupo, New Zealand, by the New Zealand Branch), p. 207–208.

De Schamphelaere, K.A.C., and Janssen, C.R., 2004, Bioavailability and chronic toxicity of zinc to juvenile rainbow trout (*Oncorhynchus mykiss*)—Comparison with other fish species and development of a biotic ligand model: Environmental Science and Technology, v. 38, no. 23, p. 6201–6209. [Also available at http://dx.doi.org/10.1021/es049720m.]

Diakonov, I.I., Pokrovski, G.S., Bénézeth, Pascale, Schott, Jacques, Dandurand, J-L., and Escalier, Jocelyne, 1997, Gallium speciation in aqueous solution—Experimental study and modelling—Part 1. Thermodynamic properties of $Ga(OH)_4^-$ to 300 ºC: Geochimica et Cosmochimica Acta,v. 61, no. 7, p. 1333–1343. [Also available at http://dx.doi.org/10.1016/S0016-7037(97)00011-2.]

Dittrich, T., Seifert, T., and Gutzmer, J., 2011, Gallium in bauxite deposits [abs]: Mineralogical Magazine, Goldschmidt Conference Abstracts 2011, v. 75, no. 3, sec. D, p. 765.

Dowa Holdings Co., Ltd., 2013, Dowa Metals and Mining—Overview of operations with a section on the zinc business and the rare metals business—Japan's largest zinc smelting plant: Tokyo, Japan, Dowa Holdings Co., Ltd., accessed February 1, 2013, at http://www.dowa.co.jp/en/jigyo/metalmine_summary.html.

Dusel-Bacon, Cynthia, Foley, N.K., Slack, J.F., Koenig, A.E., and Oscarson, R.L., 2012, Peralkaline- and calc-alkaline-hosted volcanogenic massive sulfide deposits of the Bonnifield district, east-central Alaska: Economic Geology, v. 107, p. 1403–1432. [Also available at http://dx.doi.org/10.2113/econgeo.107.7.1403.]

Dusel-Bacon, Cynthia, Slack, J.F., Koenig, A.E., Foley, N.K., Oscarson, R.L., and Gans, K.D., 2011, Whole-rock and sulfide-mineral geochemical data for samples from volcanogenic massive sulfide deposits of the Bonnifield district, east-central Alaska: U.S. Geological Survey Open-File Report 2011–1171, 43 p. [Also available at http://pubs.usgs.gov/of/2011/1171/.]

Dutrizac, J.E., Jambor, J.L., and Chen, T.T., 1986, Host minerals for the gallium-germanium ores of the Apex Mine, Utah: Economic Geology, v. 81, p. 946–950. [Also available at http://dx.doi.org/10.2113/gsecongeo.81.4.946.]

Eagleson, Mary, translator; Jakubke, H.-D., and Jeschkeit, Hans, eds., 1994, Concise encyclopedia chemistry: New York, N.Y., Walter de Gruyter, 1201 p.

Efroymson, R.A., Will, M.E., Suter, G.W., II, and Wooten, A.C., 1997, Toxicological benchmarks for screening contaminants of potential concern for effects on terrestrial plants—1997 revision, report prepared for the U.S. Department of Energy by Lockheed Martin Energy Systems, Inc.: Oak Ridge, Tenn., Oak Ridge National Laboratory, ES/ER/TM–85/R3, November, 68 p. and two appendixes, accessed March 4, 2013, at http://www.esd.ornl.gov/programs/ecorisk/documents/tm85r3.pdf.

Emsbo, Poul, 2009, Geologic criteria for the assessment of sedimentary exhalative (sedex) Zn-Pb-Ag deposits: U.S. Geological Survey Open-File Report 2009–1209, 21 p. [Also available at http://pubs.usgs.gov/of/2009/1209/.]

Emsley, John, 2001, Nature's building blocks—An A–Z guide to the elements: Oxford, United Kingdom, Oxford University Press, 538 p.

Eveleth, R.W., and Lueth, V.W., 2009, Old Hansonburg, one of New Mexico's forgotten mining camps, *in* Lueth, V.W., and others, eds., Geology of the Chupadera Mesa—New Mexico Geological Society 60th annual Field Conference, October 7–10, 2009 (1st edition): New Mexico Geological Society Field Conference, 60th, Socorro, N.M., Annual fall field conference guidebook, p. 399–406.

Finkelman, R.B., 1993, Trace and minor elements in coal, *in* Engel, M.H., and Macko, S.A., eds., Organic geochemistry—Principles and applications: New York, N.Y., Plenum Press, p. 593–607, 7 pls.

Flora, S.J.S., 2000, Possible health hazards associated with the use of toxic metals in semiconductor industries: Journal of Occupational Health, v. 42, p. 105–110. [Also available at http://dx.doi.org/10.1539/joh.42.105.]

Foley, N.K., and Ayuso, R.A., 2013, Rare earth element mobility in high-alumina altered metavolcanic deposits, South Carolina, USA: Journal of Geochemical Exploration, v. 133, p. 50–67. [Also available at http://dx.doi.org/10.1016/j.gexplo.2013.03.008.]

Foley, N.K., 2002a, Environmental chemistry of platform carbonate-hosted sulfide deposits, chap. E *of* Seal, R.R., II, and Foley, N.K., eds, Progress on geoenvironmental models for selected mineral deposit types: U.S. Geological Survey Open-File Report 02–195 (On-line version 1.0), p. 87–100.

Foley, N.K., 2002b, A geoenvironmental lifecycle model—The Austinville platform carbonate deposit, Virginia, chap. F *of* Seal, R.R., II, and Foley, N.K., eds., Progress on geoenvironmental models for selected mineral deposit types: USGS Open-File Report 02–195 (Online version 1.0), p. 101–107.

Foley, N.K., Dusel-Bacon, Cynthia, Koenig, Alan, and Schulte, Ruth, 2008, Comparative study of rare trace metals associated with massive sulfide deposits of the Bonnifield district, Alaska [abs], *in* Belkin, H.E., ed., Program and abstracts—Ninth Pan-American conference on research on fluid inclusions, in memory of Edwin Roedder—PACROFI IX—U.S. Geological Suvey, Reston, Va., USA, June 2–5, 2008: Reston, Va., U.S. Geological Survey, 64 p.

Freyssinet, P., Butt, C.R.M., Morris, R.C., and Piantone, P., 2005, Ore-forming processes related to lateritic weathering, *in* Hedenquist, J.W., Thompson, J.F.H., Goldfarb, R.J., and Richards, J.P., eds., Economic Geology—One hundredth anniversary volume, 1905–2005: Littleton, Colo., Society of Economic Geologists, p. 681–722. [Appendixes are on a CD–ROM inside the back cover.]

Frimmel, H.E., Deane, J.G., and Chadwick, P.J., 1996, Pan-African tectonism and the genesis of base metal sulfide deposits in the northern foreland of the Damara orogen, Namibia, *in* Sangster, D.F., ed., Carbonate-hosted lead-zinc deposits— [Society of Economic Geologists] 75th anniversary volume: Littleton, Colo., Society of Economic Geologists Special Publication no. 4, p. 204–217.

Fthenakis, V.M., Kim, H.C., and Alsema, Erik, 2008, Emissions from photovoltaic life cycles: Environmental Science and Technology, v. 42, no. 6, p. 2168–2174. [Also available at http://dx.doi.org/10.1021/es071763q.]

Gaillardet, J., Viers, J., and Dupré, B., 2003, Trace elements in river waters, *in* Drever, J.I., ed., Surface and groundwater, weathering, and soils, v. 5 of Holland, H.D., and Turekian, K.K., eds., Treatise on geochemistry: Oxford, United Kingdom, Elsevier-Pergamon, v. 5, p. 225–272. [Also available at http://dx.doi.org/10.1016/B0-08-043751-6/05165-3.]

Gardner, J.H., and Bell, D.T., 2007, Bauxite mining restoration by Alcoa World Alumina Australia in Western Australia—Social, political, historical, and environmental contexts: Restoration Ecology, v. 15, supplement s4, p. S3–S10. [Also available at http://dx.doi.org/10.1111/j.1526-100X.2007.00287.x.]

Goguel, R., 1988, Ultra-trace metal analysis of New Zealand geothermal waters by ICP-MS, *in* Proceedings of the Conference on Trace Elements in New Zealand—Environmental, Human and Animal, Lincoln College, Canterbury, New Zealand, November 30–December 2, 1988: New Zealand Trace Elements Group, p. 263–270.

Graedel, T.E., 2011, On the future availability of the energy metals: Annual Review of Materials Research, v. 41, p. 323–335. [Also available at http://dx.doi.org/10.1146/annurev-matsci-062910-095759.]

Graedel, T.E., Allwood, Julian, Birat, J.-P., Buchert, Matthias, Hagelüken, Christian, Reck, B.K., Sibley, S.F., and Sonnemann, Guido, 2011, What do we know about metal recycling rates?: Journal of Industrial Ecology, v. 15, no. 3, p. 355–366. [Also available at http://dx.doi.org/10.1111/j.1530-9290.2011.00342.x.]

Groves, D.I., and Bierlein, F.P., 2007, Geodynamic settings of mineral deposit systems: Journal of the Geological Society, London, United Kingdom, v. 164, no. 1, p. 19–30. [Also available at http://dx.doi.org/10.1144/0016-76492006-065.]

Gupta, V.K., Nayak, Arunima, Agarwal, Shilpi, Dobhal, Rajendra, Uniyal, D.P., Singh, Prashant, Sharma, Bhavtosh, Tyagi, Shweta, and Singh, Rakesh, 2012, Arsenic speciation analysis and remediation techniques in drinking water: Desalination and Water Treatment, v. 40, nos. 1–3, p. 231–243. [Also available http://dx.doi.org/10.1080/19443994.2012.671250].

Haest, Maarten, Muchez, Philippe, Dewaele, Stijn, Boyce, A.J., Von quadt, Albrecht, and Schneider, Jens, 2009, Petrographic, fluid inclusion and isotopic study of the Dikulushi Cu-Ag deposit, Katanga (D.R.C.)—Implications for exploration: Mineralium Deposita, v. 44, no. 5, p. 505–522. [Also available at http://dx.doi.org/10.1007/s00126-009-0230-x.]

Hagni, R.D., 1983, Minor elements in Mississippi Valley-type ore deposits—Unconventional deposits in low grade environments, chap. 7 *of* Shanks, W.C., III, ed., Cameron volume on unconventional mineral deposits: New York, N.Y., Society of Mining Engineers, p. 71–88.

Hall, W.E., and Heyl, A.V., 1968, Distribution of minor elements in ore and host rock, Illinois-Kentucky fluorite district and Upper Mississippi Valley zinc-lead district: Economic Geology, v. 63, p. 655–670. [Also available at http://dx.doi.org/10.2113/gsecongeo.63.6.655.]

Hieronymus, B., Kotschoubey, B., Boulegue, J., Benedetti, M., Godot, J.M., and Truckenbrodt, W., 1990, Aluminum behaviour in some alterites of eastern Amazonia (Brazil): Chemical Geology, v. 84, nos. 1–4, p. 74–77. [Also available at http://dx.doi.org/10.1016/0009-2541(90)90168-7.]

Hitzman, M.W., 1986, Geology of the Ruby Creek copper deposit, southwestern Brooks Range, Alaska: Economic Geology, v. 81, p. 1644–1674. [Also available at http://dx.doi.org/10.2113/gsecongeo.81.7.1644.]

Hitzman, M.W., Proffett, J.M., Jr., Schmidt, J.M., and Smith, T.E., 1986, Geology and mineralization of the Ambler district, northwestern Alaska: Economic Geology, v. 81, p. 1592–1618. [Also available at http://dx.doi.org/10.2113/gsecongeo.81.7.1592.]

Hitzman, Murray, Kirkham, Rodney, Broughton, David, Thorson, Jon, and Selley, David, 2005, The sediment-hosted stratiform copper ore system, *in* Hedenquist, J.W., Thompson, J.F.H., Goldfarb, R.J., and Richards, J.P., eds., Economic Geology—One hundredth anniversary volume—1905–2005: Littleton, Colo., Society of Economic Geologists, Inc., p. 609–642. [Appendixes are on a CD–ROM inside the back cover.]

Holecy, E.G., and Mousavi, Aliyar, 2012, Lead sources, toxicity, and human risk in children of developing countries—A mini-review: Environmental Forensics, v. 13, no. 4, p. 289–292. [Also available at http://dx.doi.org/10.1080/15275922.2012.729010.]

Hörmann, P.K., 1978, Germanium B-M, O, *in* Wedepohl, K.H., ed., Handbook of geochemistry, v. 2, pt. 3: Berlin, West Germany, Springer-Verlag, p. 31–D–10.

Hughes, M.J., 1987, The Tsumeb ore body, Namibia, and related dolostone-hosted base metal ore deposits of Central Africa: Johannesburg, South Africa, University of the Witwatersrand, Doctor of Science thesis, 448 p.

Hughes, M.J., Welke, H.J., and Allsopp, H.L, 1984, Lead isotopic studies of some Late Proterozoic stratabound ores of central Africa: Precambrian Research, v. 25, nos. 1–3, p.137–139. [Also available at http://dx.doi.org/10.1016/0301-9268(84)90029-9.]

Instytutu Problem Materialoznavstva, 1968, Handbook of the physicochemical properties of the elements: New York, N.Y., IFI-Plenum, 941 p.

Intiomale, M.M., and Oosterbosch, R., 1974, Géologie et géochmie du gisement de Kipushi, Zaire [The geology and geochemistry of the Kipushi deposit, Zaire], *in* Bartholomé, Paul, ed., Gisements stratiformes et provinces cupriféres [Stratiform copper deposits and provinces]: Liège, Belgium, Centenaire de la Société Géologique de Belgique, p. 123–164.

Jaskula, B.W., 2013a, Gallium: U.S. Geological Survey Mineral Commodity Summaries 2013, p. 58–59. [Also available at https://minerals.usgs.gov/minerals/pubs/commodity/gallium/mcs-2013-galli.pdf.]

Jaskula, B.W., 2013b, Gallium [advance release], *in* Metals and minerals: U.S. Geological Survey Minerals Yearbook 2011, v. I, p. 27.1–27.9, accessed March 1, 2013, at https://minerals.usgs.gov/minerals/pubs/commodity/gallium/myb1-2011-galli.pdf.

Johan, Z., 1988, Indium and germanium in the structure of sphalerite—An example of coupled substitution with copper: Mineralogy and Petrology, v. 39, nos. 3–4, p. 211–229. [Also available at http://dx.doi.org/10.1007/BF01163036.]

Johan, Z., Oudin, E., and Picot, P., 1983, Analogues germanifères et gallifères des silicates et oxydes dans les gisements de zinc de Pyrénées centrales, France—Argutite et carboirite, deux nouvelles espèces minérales [Germanium and gallium analogues of silicates and oxides in zinc deposits of central Pyrenees, France—Argutite and carboirite, two new mineral species]: Tschermaks Mineralogische und Petrologische Mitteilungen [Tschermak Mineralogical and Petrological Releases], v. 31, nos. 1–2, p. 97– 119.

Kabata-Pendias, Alina, and Mukherjee, A.B., 2007, Trace elements from soil to human: Berlin, Germany, Springer-Verlag, 550 p.

Kabata-Pendias, Alina, and Pendias, Henryk, 2001, Trace elements in soils and plants (3d ed.): Boca Raton, Fla., CRC Press, 413 p.

Kamona, A.F., and Günzel, A., 2007, Stratigraphy and base metal mineralization in the Otavi Mountain Land, northern Namibia—A review and regional interpretation: Gondwana Research, v. 11, no. 3, p. 396–413. [Also available at http://dx.doi.org/10.1016/j.gr.2006.04.014.]

Kaneshiro, Jess, Gaillard, Nicolas, Rocheleau, Richard, and Miller, Eric, 2010, Advances in copper-chalcopyrite thin films for solar energy conversion: Solar Energy Materials and Solar Cells, v. 94, no. 1, p. 12–16. [Also available at http://dx.doi.org/10.1016/j.solmat.2009.03.032.]

Kelley, K.D., Leach, D.L., Johnson, C.A., Clark, J.L., Fayek, M., Slack, J.F., Anderson, V.M., Ayuso, R.A., and Ridley, W.I., 2004, Textural, compositional, and sulfur isotope variations of sulfide minerals in the Red Dog Zn-Pb-Ag deposits, Brooks Range, Alaska—Implications for ore formation: Economic Geology, v. 99, p. 1509–1532. [Also available at http://dx.doi.org/10.2113/99.7.1509.]

Kelley, K.D., Seal, R.R., II, Schmidt, J.M., Hoover, D.B., and Klein, D.P., 1995, Sedimentary exhalative Zn-Pb-Ag deposits (Model 31a; Briskey, 1986), chap. 29 *of* du Bray, E.A., ed., Preliminary compilation of descriptive geoenvironmental mineral deposit models: U.S. Geological Survey Open-File Report 95–831, p. 225–233. [Also available at http://pubs.usgs.gov/of/1995/ofr-95-0831/.

Kesler, S.E., and Reich, M.H., 2006, Precambrian Mississippi Valley-type deposits—Relation to changes in composition of the hydrosphere and atmosphere, *in* Kesler, S.A., and Ohmoto, Hiroshi, eds., Evolution of early Earth's atmosphere, hydrosphere, and biosphere—Constraints from ore deposits: Boulder, Colo., Geological Society of America, Geological Society of America Memoir, v. 198, p. 185−204.

Khashgerel, Bat-Erdene, Kavalieris, Imants, and Hayashi, Kenichiro, 2008, Mineralogy, textures, and whole- rock geochemistry of advanced argillic alteration—Hugo Dummett porphyry Cu-Au deposit, Oyu Tolgoi mineral district, Mongolia: Mineralium Deposita, v. 43, no. 8, p. 913–932. [Also available at http://dx.doi.org/10.1007/s00126-008-0205-3.]

Kim, H.C., Fthenakis, Vasilis, Choi, J.-K., and Turney, D.E., 2012, Life cycle greenhouse gas emissions of thin-film photovoltaic electricity generation: Journal of Industrial Ecology, v. 16, Supplement S1, p. s110−s121. [Also available at http://dx.doi.org/10.1111/j.1530-9290.2011.00423.x.]

Koljonen, T., ed., 1992, Suomen Geokemian Atlas, osa 2—Moreeni [The geochemical atlas of Finland, Part 2—Till]: Espoo, Finland, Geological Survey of Finland, p. 106–125.

Krämer, V., Hirth, H., Hofherr, M., and Trah, H.-P., 1987, Phase studies in the systems Ag_2Te–Ga_2Te_3, ZnSe–In_2Se_3 and ZnS–Ga_2S_3: Thermochimica Acta, v. 112, no. 1, p. 89–94.

Large, D.E., 1981, The geochemistry of sedimentary rocks in the vicinity of the Tom Pb-Zn-Ag deposit, Yukon Territory, Canada: Journal of Geochemical Exploration, v. 15, nos. 1–3, p. 203–217. [Also available at http://dx.doi.org/10.1016/0375-6742(81)90063-7.]

Large, D.E., 1983, Sediment-hosted massive sulphide lead-zinc deposits—An empirical model, *in* Sangster, D.F., ed., Sediment-hosted stratiform lead-zinc deposits—A short course sponsored by the Mineralogical Association of Canada and held immediately prior to the 1983 annual meeting in Victoria, B.C., May 11–13: Mineralogical Association of Canada Short Course Series, v. 9, p. 1–29.

Large, R.R., Bull, S.W., McGoldrick, P.J., Derrick, G.M., Carr, G.R., and Walters, Steve, 2005, Stratiform and strata-bound Zn-Pb-Ag deposits of the Proterozoic sedimentary basins of northern Australia, *in* Hedenquist, J.W., Thompson, J.F.H., Goldfarb, R.J., and Richards, J.P., eds., Economic Geology—One hundredth anniversary volume, 1905–2005: Littleton, Colo., Society of Economic Geologists, p. 931−963. [Appendixes are on a CD–ROM inside the back cover.]

Lavery, N.G., Leach, D.L., and Saunders, J.A., 1994, Lithogeochemical investigations applied to exploration for sediment-hosted lead-zinc deposits, *in* Fontboté, Lluis, and Boni, Maria, eds., Sediment-hosted Zn-Pb ores—Society for Geology Applied to Mineral Deposits special publication: New York, N.Y., Springer–Verlag, v. 10, p. 393–428.

Leach, D.L., and Sangster, D.F., 1993, Mississippi Valley-type lead-zinc deposits, *in* Kirkham, R.V., Sinclair, W.D., Thorpe, R.I., and Duke, J.M., eds., Mineral deposit modeling: International Conference on Mineral Deposit Modeling, Ottawa, Ontario, Canada, 1990, Geological Association of Canada Special Paper 40, p. 289−314.

Leach, D.L., Bradley, D.C., Huston, D.L., Pisarevsky, S.A., Taylor, R.D., and Gardoll, S.J., 2010, Sediment-hosted lead-zinc deposits in Earth history: Economic Geology, v. 105, p. 593–625. [Also available at http://dx.doi.org/10.2113/gsecongeo.105.3.593.]

Leach, D.L., Bradley, Dwight, Lewchuk, M.T., Symons, D.T.A., de Marsily, Ghislain, and Brannon, Joyce, 2001, Mississippi Valley-type lead-zinc deposits through geological time—Implications from recent age-dating research: Mineralium Deposita, v. 36, no. 8, p. 711−740. [Also available at http://dx.doi.org/10.1007/s001260100208.]

Leach, D., Marsh, E., Bradley, D., Gardoll, S., and Huston, D., 2005, The distribution of SEDEX Pb-Zn deposits through Earth history, *in* Mao, Juingwen and Bierlein, F.P., eds., Mineral deposit research—Meeting the global challenge—Proceedings of the Eighth Biennial SGA Meeting, Beijing, China, August 18–21, 2005: Heidelberg, Switzerland, Society for Geology Applied to Mineral Deposits, p. 145−149.

Leach, D.L., Marsh, Erin, Emsbo, Poul, Rombach, C.S., Kelley, K.D., Reynolds, Jim, and Anthony, Mike, 2004, Nature of hydrothermal fluids at the shale-hosted Red Dog Zn-Pb-Ag deposits, Brooks Range, Alaska: Economic Geology, v. 99, p. 1449−1480. [Also available at http://dx.doi.org/10.2113/gsecongeo.99.7.1449.]

Leach, D.L., Sangster, D.F., Kelley, K.D., Large, R.R., Garven, Grant, Allen, C.R., Gutzmer, Jens, and Walters, Steve, 2005, Sediment-hosted lead-zinc deposits—A global perspective, *in* Hedenquist, J.W., Thompson, J.F.H., Goldfarb, R.J., and Richards, J.P., eds., Economic Geology—One hundredth anniversary volume, 1905–2005: Littleton, Colo., Society of Economic Geologists, p. 561−607. [Appendixes are on a CD–ROM inside the back cover.]

Leach, D.L., Taylor, R.D., Fey, D.L., Diehl, S.F., and Saltus, R.W., 2010, A deposit model for Mississippi Valley-type lead-zinc ores, chap. A *of* Mineral deposit models for resource assessment: U.S. Geological Survey Scientific Investigations Report 2010–5070–A, 52 p.

Leach, D.L., Viets, J.B., Foley-Ayuso, Nora, and Klein, D.P., 1995, Mississippi Valley-type Pb-Zn deposits (Models 32a, b; Briskey, 1986a, b), chap. 30 *of* du Bray, E.A., ed., Preliminary compilation of descriptive geoenvironmental mineral deposit models: U.S. Geological Survey Open-File Report 95–831, p. 234–243. [Also available at http://pubs.usgs.gov/of/1995/ofr-95-0831/.]

Lide, D.R., ed., 2005, CRC handbook of chemistry and physics (86th ed.): Boca Raton, Fla., CRC Press, 2,544 p.

Lottermoser, B.G., 2010, Mine wastes—Characterization, treatment, and environmental impacts (3d ed.): Berlin, Germany, Springer-Verlag, 400 p. [Also available at http://dx.doi.org/10.1007/978-3-642-12419-8.]

Lydon, J.W., 1983, Chemical parameters controlling the origin and deposition of sediment-hosted stratiform lead-zinc deposits, *in* Sangster, D.F., ed., Sediment-hosted stratiform lead-zinc deposits—A short course sponsored by the Mineralogical Association of Canada and held immediately prior to the 1983 annual meeting in Victoria, B.C., May 11–13: Mineralogical Association of Canada Short Course Series, v. 9, p. 175−250.

Macdonald, Ray, and Bailey, D.K., 1973. Chemistry of igneous rocks—Part 1, The chemistry of the peralkaline oversaturated obsidians: U.S. Geological Survey Professional Paper 440 N–1, 36 p.

Mastalerz, Maria, and Drobniak, Agnieszka, 2012, Gallium and germanium in selected Indiana coals: International Journal of Coal Geology, v. 94, p. 302–313. [Also available at http://dx.doi.org/10.1016/j.coal.2011.09.007.]

Max Planck Institute, 2002, Geochemistry of rocks of the oceans and continents database (GEOROC): Max Planck Institute for Chemistry database, accessed March 1, 2013, at http://georoc.mpch-mainz.gwdg.de/.

Mayes, W.M., Jarvis, A.P., Burke, I.T., Walton, Melanie, Feigl, Viktória, Klebercz, Orsolya, and Gruiz, Katalin, 2011, Dispersal and attenuation of trace contaminants downstream of the Ajka bauxite residue (red mud) depository failure, Hungary: Environmental Science and Technology, v. 45, p. 5147–5155. [Also available at http://dx.doi.org/10.1021/es200850y.]

McDermott, R.K., and Sibley, J.M., 2000, The Aznalcóllar tailings dam accident—A case study: Mineral Resources Engineering, v. 9, no. 1, p. 101–118.

McFarlane, M.J., 1976, Laterite and landscape: New York, N.Y., Academic Press, 151 p., 4 pls.

McLennan, S.M., and Murray, R.W., 1999, Geochemistry of sediments, *in* Marshall, C.P., and Fairbridge, R.W., eds., Encyclopedia of geochemistry: Boston, Mass., Kluwer Academic, p. 282–292.

Melcher, F., Oberthur, R., and Rammalmair, D., 2006, Geochemical and mineralogical distribution of germanium in the Khusib Springs Cu–Zn–Pb–Ag sulfide deposit, Otavi Mountain Land, Namibia: Ore Geology Reviews, v. 28, p. 32–56.

Melfos, Vasilios, and Voudouris, P.Ch., 2012, Geological, mineralogical, and geochemical aspects for critical and rare metals in Greece: Minerals, v. 2, no. 4, p. 300–317. [Also available at http://dx.doi.org/10.3390/min2040300.]

Mendeleev, Dmitri, 1871, The periodical regularity of the chemical elements: Annalen der Chemie und Pharmacie, Supplement-band, v. 8, p. 133–229.

Metal Bulletin, 2013, China and minor metals—What next?: Metal Bulletin, May 10, accessed May 19, 2013 at http://www.metalbulletin.com/Article/3195423/China-and-minor-metalswhat-next.html.

Mielke, J.M., 1979, Composition of the Earth's crust and distribution of the elements, *in* International Association of Geochemistry and Cosmochemistry, Review of research on modern problems in geochemistry, v. 16: Paris, France, United Nations Educational, Scientific and Cultural Organization, p. 13–39.

Miles, R.W., Zoppi, Guillaume, and Forbes, Ian, 2007, Inorganic photovoltaic cells: Materials Today, v. 10, no. 11, p. 20 –27. [Also available at http://dx.doi.org/10.1016/S1369-7021(07)70275-4.]

Misiewicz, J.E., 1988, The geology and metallogeny of the Otavi Mountain Land, Damara Orogen, SWA/Namibia, with particular reference to the Berg Aukas Zn-Pb-V deposit—A model of ore genesis: Grahamstown, South Africa, Rhodes University, Master of Science Dissertation, 143 p. [Maps and illustrations.]

Moskalyk, R.R., 2003, Gallium—The backbone of the electronics industry: Minerals Engineering, v. 16, no. 10, p. 921–929. [Also available at http://dx.doi.org/10.1016/j.mineng.2003.08.003.]

Nagajyoti, P.C., Lee, K.D., and Sreekanth, T.V.M., 2010, Heavy metals, occurrence and toxicity for plants—A review: Environmental Chemistry Letters, v. 8, no. 3, p. 199–216. [Also available at http://dx.doi.org/10.1007/s10311-010-0297-8.]

Natural Earth, 2014, Small scale data: Natural Earth map dataset, scale 1:110,000,000, accessed June 23, 2014, at http://www.naturalearthdata.com.

Onikura, N., Nakamura, A., and Kishi, K., 2005, Acute toxicity of gallium and effects of salinity on gallium toxicity to brackish and marine organisms: Bulletin of Environmental Contamination and Toxicology, v. 75, no. 2, p. 356–360. [Also available at http://dx.doi.org/10.1007/s00128-005-0761-5.]

Orians, K.J., and Bruland, K.W., 1988, The marine geochemistry of dissolved gallium—A comparison with dissolved aluminum: Geochimica et Cosmochimica Acta, v. 52, no. 12, p. 2955–2962. [Also available at http://dx.doi.org/10.1016/0016-7037(88)90160-3.]

Parrotta, J.A., Knowles, O.H., and Wunderle, J.M., Jr., 1997, Development of floristic diversity in 10-year-old restoration forests on a bauxite mined site in Amazonia: Forestry Ecology and Management, v. 99, nos. 1–2, p. 21–42.

Patterson, S.H., Kurtz, H.F., Olson, J.C., and Neeley, C.L., 1986, World bauxite resources: U.S. Geological Survey Professional Paper 1076–B, 151 p. [Also available at http://pubs.er.usgs.gov/publication/pp1076B.] .

Pearson, R.G., 1963, Hard and soft acids and bases: Journal of the American Chemical Society, v. 85, no. 22, p. 3533–3539. [Also available at http://dx.doi.org/10.1021/ja00905a001.]

Plumlee, G.S,. and Logsdon, M.J., 1999, An Earth-system science toolkit for environmentally friendly mineral resource development, *in* Plumlee, G.S. and Logsdon, M.J., eds., The environmental geochemistry of mineral deposits—Part A, Processes, techniques, and health issues: Littleton, Colo., Society of Economic Geologists, v. 1, p. 1–27.

Plumlee, G.S., Smith, K.S., Montour, M.R., Ficklin, W.H., and Mosier, E.L., 1999, Geological controls on the composition of natural waters and mine waters draining diverse mineral-deposit types, *in* Plumlee, G.S. and Filipek, L.H., eds., The environmental geochemistry of mineral deposits—Part B, Case studies and research topics: Littleton, Colo., Society of Economic Geologists, Reviews in Economic Geology Series, v. 6B, p. 373–432. [Also available at http://ebooks.geoscienceworld.org/content/the-environmental-geochemistry-of-mineral-deposits.]

Połedniok, J., Andrzej, K., and Zerzucha, P., 2012, Spectrophotometric and inductively coupled plasma-optical emission spectroscopy determination of gallium in natural soils and soils polluted by industry—Relationships between elements: Communications in Soil Science and Plant Analysis, v. 43, no. 8, p. 1121–1135. [Also available at http://dx.doi.org/10.1080/00103624.2012.662561.]

Rambaldi, E.R., Rajan, R.S., Housley, R.M., and Wang, D., 1986, Gallium-bearing sphalerite in a metal- sulfide nodule of the Qingzhen (EH3) chondrite: Meteoritics, v. 21, p. 23–31.

Reck, B.K., and Graedel, T.E., 2012, Challenges in metal recycling: Science, v. 337, no. 6095, p. 690–695. [Also available at http://dx.doi.org/10.1126/science.1217501.]

Reeves, H.J., Wealthall, G., and Younger, P.L., 2011, Advisory visit to the bauxite processing tailings dam near Ajka, Veszprém County, western Hungary: Keyworth, United Kingdom, British Geological Survey Open Report OR/11/006.

Rêserva International LLC, 2008, Executive summary of the "NI 43-101 Technical Report and Resource Estimation for the Cordero Gallium Project, Humboldt County, Nevada, USA," prepared for Gold Canyon Resources, Inc.: Reno, Nev., Rêserva International LLC, January, 2 p.

Retallack, G.J., 2010, Lateritization and bauxitization events: Economic Geology, v. 105, p. 655–667. [Also available at http://dx.doi.org/10.2113/gsecongeo.105.3.655.]

Riley, J.P., 1961, Composition of mineral water from the hot spring at Bath: Journal of Applied Geochemistry, v. 11, p. 190–191.

Rockett, A.A., 2010, Current status and opportunities in chalcopyrite solar cells: Current Opinion in Solid State and Materials Science, v. 14, no. 6, p. 143–148. [Also available at http://dx.doi.org/10.1016/j.cossms.2010.08.001.]

Rudnick, R.L., and Gao, S., 2003, Composition of the continental crust, *in* Rudnick, R.L., ed., The crust, v. 3 of Holland, H.D., and Turekian, K.K., eds., Treatise on geochemistry: Oxford, United Kingdom, Elsevier-Pergamon, p. 1–64. [Also available at http://dx.doi.org/10.1016/B0-08-043751-6/03016-4.]

Ruyters, S., Mertens, J., Vassilieva, E., Dehandschutter, B., Poffijn, A., and Smolders, E., 2011, The red mud accident in Ajka (Hungary)—Plant toxicity and trace metal bioavailability in red mud contaminated soil: Environmental Science and Technology, v. 45, no. 4, p. 1616–1622. [Also available at http://dx.doi.org/10.1021/es104000m.]

Rytuba, J.J., John, D.A., Foster, Andrea, Ludington, S.D., and Kotlyar, Boris, 2003, Hydrothermal enrichment of gallium in zones of advanced argillic alteration—Examples from the Paradise Peak and McDermitt ore deposits, Nevada, chap. C *of* Contributions to industrial-minerals research: U.S. Geological Survey Bulletin 2209–C, accessed January 1, 2012, at http://pubs.usgs.gov/bul/b2209/.

Salminen, R., ed., 2015, Geochemical atlas of Europe—Part 1, Background information, methodology, and maps: Espoo, Finland, Geological Survey of Finland database, accessed September 25, 2015, at http://weppi.gtk.fi/publ/foregsatlas/index.php.

Sangster, D.F., 1990, Mississippi Valley-type and sedex lead-zinc deposits—A comparative examination: Transactions of the Institution of Mining and Metallurgy, Section B—Applied Earth Science, v. 99, p. B21−B42.

Schlüter, Jochen, Klaska, K.-H., Adiwidjaja, Gunadi, and Gebhard, Georg, 2003, Tsumgallite, GaO(OH), a new mineral from the Tsumeb Mine, Tsumeb, Namibia: Neues Jahrbuch für Mineralogie–Monatshefte, v. 2003, no. 11, p. 521–527. [Also available at http://dx.doi.org/10.1127/0028-3649/2003/2003-0521.]

Schneider, J., Melcher, F., and Brauns, M., 2007, Concordant ages for the giant Kipushi base metal deposit (DR Congo) from direct Rb-Sr and Re-Os dating of sulfides: Mineralium Deposita, v. 42, no. 7, p. 791–797. [Also available at http://dx.doi.org/10.1007/s00126-007-0158-y.]

Schroll, Erich, 1999, Gallium—Element and geochemistry, *in* Marshall, C.P., and Fairbridge, R.W., eds., Encyclopedia of geochemistry: Boston, Mass., Kluwer, p. 257–259.

Schruben, Paul, 2002, Assessment of undiscovered deposits of gold, silver, copper, lead, and zinc in the United States—A portable document (pdf) recompilation of USGS OFR 96–96 and Circular 1178: U.S. Geological Survey Open-File Report 2002–198.

Schulte, R.F., and Foley, N.K., 2014, Compilation of gallium resource data for bauxite deposits: U.S. Geological Survey Open-File Report 2013–1272, 14 p., 3 separate tables. [Also available at http://dx.doi.org/10.3133/ofr20131272.]

Selby, David, Kelley, K.D., Hitzman, M.W., and Zieg, Jerry, 2009, Re-Os sulfide (bornite, chalcopyrite, and pyrite) systematics of the carbonate-hosted copper deposits at Ruby Creek, southern Brooks Range, Alaska: Economic Geology, v. 104, p. 437–444. [Also available at http://dx.doi.org/10.2113/gsecongeo.104.3.437.]

Shacklette, H.T., and Boerngen, J.G., 1984, Element concentrations in soils and other surficial materials of the conterminous United States: U.S. Geological Survey Professional Paper 1270, 105 p. [Also available at http://pubs.usgs.gov/pp/1270/.]

Shanks, W.C., III, and Thurston, Roland, eds., 2012, Volcanogenic massive sulfide occurrence model—chap. C *of* Mineral deposit models for resource assessment: U.S. Geological Survey Scientific Investigations Report 2010–5070–C, 345 p. [Also available at http://pubs.usgs.gov/sir/2010/5070/c/.]

Shannon, R.D., 1976, Revised effective ionic radii and systematic studies of interatomic distances in halides and chalcogenides: Acta Crystallographica Section A—Foundations, v. 32, no. 5, p. 751–767.

Shiller, A.M., 1998, Dissolved gallium in the Atlantic Ocean: Marine Chemistry, v. 61, nos. 1–2, p. 87–99. [Also available at http://dx.doi.org/10.1016/S0304-4203(98)00009-7.]

Shiller, A.M., and Frilot, D.M., 1996, The geochemistry of gallium relative to aluminum in Californian streams: Geochimica et Cosmochimica Acta, v. 60, no. 8, p. 1323–1328. [Also available at http://dx.doi.org/10.1016/0016-7037(96)00002-6.]

Smith, K.S., and Huyck, H.L.O., 1999, An overview of the abundance, relative mobility, bioavailability, and human toxicity of metals, *in* Plumlee, G.S., and Logsdon, M.J, eds., The environmental geochemistry of mineral deposits—Part A, Processes, techniques and health issues: Littleton, Colo., Society of Economic Geologists, v. 1, p. 29–70.

Söhnge, P.G., 1964, The geology of the Tsumeb Mine, *in* Haughton, S.H., ed., The geology of some ore deposits in southern Africa, v. 2: Johannesburg, South Africa, Geological Society of South Africa, p. 367–382.

Soler, J.M., and Lasaga, A.C., 1996, A mass transfer model of bauxite formation: Geochimica et Cosmochimica Acta, v. 60, no. 24, p. 4913–4931. [Also available at http://dx.doi.org/10.1016/S0016-7037(96)00319-5.]

SRK Consulting (Canada) Inc., 2007, Red Dog Mine closure and reclamation plan—SD B3—Plan of operations for tailings and water management—Report prepared for Teck Cominco Alaska, Inc.: Vancouver, British Columbia, Canada, SRK Consulting (Canada) Inc., SRK Project Number 1CT006.003, 8 p. [Also available at http://dnr.alaska.gov/mlw/mining/largemine/reddog/publicnotice/pdf/sdb3.pdf.]

Suter, G.W., II, and Tsao, C.L., 1996, Toxicological benchmarks for screening potential contaminants of concern for effects on aquatic biota—1996 revision: Oak Ridge, Tenn., Lockheed Martin Energy Systems Inc., ES/ER/TM-96/R2, variously paged, accessed March 4, 2013, at http://www.esd.ornl.gov/programs/ecorisk/documents/tm96r2.pdf.

Taylor, R.D., Leach, D.L., Bradley, D.C., and Pisarevsky, S.A., 2009, Compilation of mineral resource data for Mississippi Valley-type and clastic-dominated sediment-hosted lead-zinc deposits: U.S. Geological Survey Open-File Report 2009–1297, 42 p.

Taylor, S.R., and McLennan, S.M., 1995, The geochemical evolution of the continental crust: Reviews of Geophysics, v. 33, no. 2, p. 241–265. [Also available at http://dx.doi.org/10.1029/95RG00262.]

Tervek, R.W., and Fay, J.E., 1986, Gallium—An overview, markets, supplies and occurrence, *in* Elliott, I.L., and Smee, B.W., GEOEXPO/86—Exploration in the North American Cordillera—Proceedings of a symposium jointly sponsored by the Association of Exploration Geochemists and the Cordilleran Section, Geological Association of Canada, University of British Columbia, Vancouver, B.C., Canada, May 12th–14th, 1986: Vancouver, British Columbia, Canada, Geological Association of Canada, p. 209–212.

Tolcin, A.C., 2013, Zinc: U.S. Geological Survey Mineral Commodity Summaries 2013, p. 188–189. [Also available at https://minerals.usgs.gov/minerals/pubs/commodity/zinc/mcs-2013-zinc.pdf.]

Trenfield, M.A., Markich, S.J., Ng, J.C., Noller, B., and van Dam, R.A., 2012, Dissolved organic carbon reduces the toxicity of aluminum to three tropical freshwater organisms: Environmental Toxicology and Chemistry, v. 31, no. 2, p. 427–436. [Also available at http://dx.doi.org/10.1002/etc.1704.]

Tyler, Germund, 2004, Vertical distribution of major, minor, and rare elements in a Haplic Podzol: Geoderma, v. 119, nos. 3–4, p. 277–290. [Also available at http://dx.doi.org/10.1016/j.geoderma.2003.08.005.]

Ueno, TeIchi, and Scott, S.D., 2002, Phase equilibria in the system Zn-Fe-Ga-S at 900 ºC and 800 ºC: The Canadian Mineralogist, v. 40, p. 563–570. [Also available at http://dx.doi.org/10.2113/gscanmin.40.2.563.]

U.S. Environmental Protection Agency, 2006, Assessment of the potential costs, benefits, and other impacts of chat use in transportation projects: Washington, D.C., U.S. Environmental Protection Agency, Office of Solid Waste, Reference no. S.2006.1, 81 p.

U.S. Environmental Protection Agency, 2010, Record of Decision by the U.S. Environmental Protection Agency Region 10 for the Red Dog Mine Extension Aqqaluk Project: Washington, D.C., U.S. Environmental Protection Agency, 15 p. [Also available at http://www.epa.gov/region10/pdf/permits/npdes/ak/red-dog-aqqaluk-rod.pdf.]

U.S. Environmental Protection Agency, 2013a, National ambient air quality standards (NAAQS)—Lead (Pb) standards—Table of historical Pb NAAQS: U.S. Environmental Protection Agency, accessed February 18, 2013, at http://www.epa.gov/ttn/naaqs/standards/pb/s_pb_history.html.

U.S. Environmental Protection Agency, 2013b, National primary drinking water regulations: U.S. Environmental Protection Agency, EPA 816–F–09–004, May, 6 p., accessed February 15, 2013, at http://water.epa.gov/drink/contaminants/index.cfm.

U.S. Geological Survey, 1996, Global 30 arc-second elevation (GTOPO30): Reston, Va., U.S. Geological Survey dataset (digital elevation model), accessed June 23, 2014, at https://lta.cr.usgs.gov/GTOPO30.

U.S. Natural Resources Conservation Service, Soil Survey Staff, 2000, Keys to soil taxonomy: Blacksburg, Virginia, Pocahontas Press, 600 p.

Uzumasa, Y., and Nasu, Y., 1960, Chemical investigations of hot springs in Japan: LVII. Gallium in hot springs. Nippon Kagaku Zasshi, v. 81, p. 732.

Valeton, Ida, 1972, Bauxites: New York, N.Y., Elsevier, 206 p.

Valeton, Ida, 1983, Paleoenvironment of lateritic bauxites with vertical and lateral differentiation, *in* Wilson, R.C.L., ed., Residual deposits—Surface-related weathering processes and materials: London, United Kingdom, Geological Society of London, Special Publication, v. 11, p. 77–90.

van Wilderode, J., Heijlen, W., De Muynck, D., Schneider, J., Vanhaecke, F., and Muchez, Ph., 2012, The Kipushi Cu–Zn deposit (DR Congo) and its host rocks—A petrographical, stable isotope (O, C) and radiogenic isotope (Sr, Nd) study: Journal of African Earth Sciences, v. 79, p. 143–156. [Also available at http://dx.doi.org/10.1016/j.jafrearsci.2012.11.011.]

Viers, Jérôme, Dupré, Bernard, and Gaillardet, Jérôme, 2009, Chemical composition of suspended sediments in world rivers—New insights from a new database: Science of the Total Environment, v. 407, no. 2, p. 853–868. [Also available at http://dx.doi.org/10.1016/j.scitotenv.2008.09.053.]

Viets, J.G., Hopkins, R.T., and Miller, B.M., 1992, Variations in minor and trace metals in sphalerite from Mississippi Valley-type deposits of the Ozark region—Genetic implications: Economic Geology, v. 97, p. 1897–1905. [Also available at http://dx.doi.org/10.2113/gsecongeo.87.7.1897.]

Washington County Historical Society, 2013, Apex Mine (aka Pen Mine, Dixie Apex Mine, Utah-Eastern Mine): St. George, Utah, Washington County Historical Society Web page, accessed September 26, 2015, at http://wchsutah.org/mining/apex-mine.php.

Weeks, R.A., 1973, Gallium, germanium, and indium, *in* Brobst, D.A., and Pratt, W. P., eds., United States mineral resources: U.S. Geological Survey Professional Paper 820, p. 237–246. [Also available at http://pubs.er.usgs.gov/publication/pp820.]

Wilkinson, B.H., McElroy, B.J., Kesler, S.E., Peters, S.E., and Rothman, E.D., 2009, Global geologic maps are tectonic speedometers—Rates of rock cycling from area-age frequencies: Geological Society of America Bulletin, v. 121, nos. 5–6, p. 760–779. [Also available at http://dx.doi.org/10.1130/B26457.1.]

Wood, S.A., and Samson, I.M., 2006, The aqueous geochemistry of gallium, germanium, indium, and scandium: Ore Geology Reviews, v. 28, no. 1, p. 57–102. [Also available at http://dx.doi.org/10.1016/j.oregeorev.2003.06.002.]

Ye, Lin, Cook, N.J., Ciobanu, C.L., Yuping, Liu, Qian, Zhang, Tiegeng, Liu, Wei, Gao, Yulong, Yang, and Danyushevskiy, Leonid, 2011, Trace and minor elements in sphalerite from base metal deposits in South China—A LA-ICPMS study: Ore Geology Reviews, v. 39, no. 4, p. 188–217. [Also available at http://dx.doi.org/10.1016/j.oregeorev.2011.03.001.]

Ziegler, T.L., Divine, K.K. and Goering, P.L., 2004, Gallium, chap. 9 *of* Merian, E., Anke, Manfred, Ihnat, Milan, and Stoeppler, Markus, eds., Elements and their compounds in the environment—Occurrence, analysis and biological relevance: Weinheim, Germany, Wiley-VCH Verlag, v. 2, p. 775–786. [Also available at http://dx.doi.org/10.1002/9783527619634.ch30.]

For more information concerning this report, please contact:
Mineral Resources Program Coordinator
U.S. Geological Survey
913 National Center
Reston, VA 20192
Telephone: 703–648–6100
Fax: 703–648–6057
Email: minerals@usgs.gov
Home page: https://minerals.usgs.gov

Prepared by the USGS Science Publishing Network
Reston Publishing Service Center
Edited by J.C. Ishee and Stokely J. Klasovsky
Illustrations by Caryl J. Wipperfurth
Layout by Caryl J. Wipperfurth and Cathy Y. Knutson
Posting by Angela E. Hall

ISSN 2330-7102 (online)
https://doi.org/10.3133/pp1802H